

# Homological mirror symmetry for toric orbifolds of toric del Pezzo surfaces

Kazushi Ueda and Masahito Yamazaki

## Abstract

We propose a mathematical formulation of the algorithm of Hanany and Vegh [22] to associate quivers with relations to lattice polygons. We study the case of toric del Pezzo surfaces in detail and discuss its relation with coamoebas following Feng, He, Kennaway and Vafa [10]. As an application, we prove homological mirror symmetry for orbifolds of toric del Pezzo surfaces by finite subgroups of the torus.

## 1 Introduction

The lattice of vanishing cycles equipped with the intersection form is called the *Milnor lattice*. It is a fundamental object in singularity theory related to other fields of mathematics such as generalizations of root systems (see e.g. [33]) and monodromy of hypergeometric functions. The Milnor lattice admits a categorification called the *directed Fukaya category*, defined by Seidel [35] based on the idea of Kontsevich [27]. Although they are important invariants in singularity theory, it is often difficult to compute the Milnor lattice of a given holomorphic function, let alone its directed Fukaya category.

Recent advances in string theory has given a significant progress in the case of Laurent polynomials in two variables. For a Laurent polynomial

$$W(x, y) = \sum_{(i, j) \in \mathbb{Z}^2} a_{ij} x^i y^j,$$

its Newton polygon  $\Delta \subset \mathbb{R}^2$  is defined as the convex hull of  $(i, j) \in \mathbb{Z}^2$  such that  $a_{ij} \neq 0$ ;

$$\Delta := \text{Conv}\{(i, j) \in \mathbb{Z}^2 \mid a_{ij} \neq 0\}.$$

Hanany and Vegh [22] introduced an algorithm to associate bipartite graphs on a real 2-torus  $T = \mathbb{R}^2/\mathbb{Z}^2$  to convex lattice polygons. See also [13, 14, 21] for earlier papers which layed the groundwork for Hanany and Vegh. Such bipartite graphs are called *brane tilings*, and encode the information of quivers with relations.

Now assume that the origin is in the interior of  $\Delta$  and consider the toric Fano stack  $X_\Delta$  defined as follows: Let  $\{v_i\}_{i=1}^N$  be the set of vertices of  $\Delta$  numbered clockwise and  $K \subset (\mathbb{C}^\times)^N$  be the kernel of the map

$$\varphi \otimes_{\mathbb{Z}} \mathbb{C}^\times : (\mathbb{C}^\times)^N \rightarrow (\mathbb{C}^\times)^2,$$

where  $\varphi : \mathbb{Z}^N \rightarrow \mathbb{Z}^2$  is a homomorphism sending the  $i$ -th coordinate vector  $e_i \in \mathbb{Z}^N$  to  $v_i$ . Put  $U = \{(x_1, x_2, x_3) \in \mathbb{C}^3 \mid (x_1, x_2, x_3) \neq (0, 0, 0)\}$  if  $N = 3$  and  $U = \{(x_i)_{i=1}^N \in \mathbb{C}^n \mid (x_i, x_j) \neq (0, 0) \text{ if } |i - j| > 1\}$  if  $N \geq 4$ . Then  $X_\Delta$  is the quotient stack

$$X_\Delta = [U/K]$$

of  $U$  by the natural action

$$\begin{array}{ccc} K & \curvearrowright & U & \rightarrow & U \\ \Downarrow & & \Downarrow & & \Downarrow \\ (\alpha_1, \dots, \alpha_N) & : & (x_1, \dots, x_N) & \mapsto & (\alpha_1 x_1, \dots, \alpha_N x_N) \end{array}$$

of  $K$ . In this situation, Hanany, Herzog and Vegh [20] proposed a method to produce a collection  $(E_1, \dots, E_M)$  of line bundles on  $X_\Delta$ , which conjecturally gives a full strong exceptional collection whose total morphism algebra  $\bigoplus_{i,j=1}^M \text{Hom}(E_i, E_j)$  is isomorphic to the path algebra of the quiver with relations obtained from  $\Delta$  through the algorithm of Hanany and Vegh. This conjecture, together with a theorem of Bondal [6, Theorem 6.2], implies that the derived category of coherent sheaves on  $X_\Delta$  is equivalent as a triangulated category to the derived category of finitely-generated right modules over the path algebra.

On the other hand, Feng, He, Kennaway, and Vafa [10] interpreted brane tilings as spines of the coamoebas of  $W^{-1}(0)$ , just as tropical curves are spines of amoebas [9, 30, 31]. Here, the *coamoeba* of a subvariety of the torus  $(\mathbb{C}^\times)^2$  is defined by Passare and Tsikh as its image under the argument map

$$\begin{array}{ccc} \text{Arg} & : & (\mathbb{C}^\times)^2 & \rightarrow & (\mathbb{R}/\mathbb{Z})^2 \\ & & \Downarrow & & \Downarrow \\ & & (x, y) & \mapsto & \frac{1}{2\pi}(\arg(x), \arg(y)). \end{array} \tag{1}$$

Feng et al. conjectured that the vanishing cycles of  $W$  correspond to faces of brane tilings by the argument map, so that the directed Fukaya category  $\mathfrak{Fuk}^{\rightarrow} W$  is derived-equivalent to the category of modules over the path algebra of the quiver with relations obtained from  $\Delta$  through the algorithm of Hanany and Vegh. This conjecture, together with the conjecture of Hanany, Herzog and Vegh in the last paragraph, implies *homological mirror symmetry* conjectured by Kontsevich [26, 27] for toric Fano stacks in dimension two.

In this paper, we propose a mathematical formulation of the algorithm of Hanany and Vegh and discuss its relation with coamoebas following Feng, He, Kennaway and Vafa. We study the case when  $X_\Delta$  is a toric del Pezzo surface in detail and prove the following:

**Theorem 1.** *Let  $W$  be a generic Laurent polynomial with the Newton polygon  $\Delta$  such that  $X_\Delta$  is a toric del Pezzo surface. Then the following hold:*

1. *The algorithm of Hanany and Vegh associates to  $\Delta$  a unique quiver  $\Gamma$  with relations.*
2. *The derived category  $D^b \text{mod } \mathbb{C}\Gamma$  of finitely-generated right modules over the path algebra  $\mathbb{C}\Gamma$  with relations is equivalent as a triangulated category to the derived category  $D^b \text{coh } K_\Delta$  of coherent sheaves on the total space of the canonical bundle  $K_\Delta$  of  $X_\Delta$ ;*

$$D^b \text{mod } \mathbb{C}\Gamma \cong D^b \text{coh } K_\Delta.$$

3. *There are as many as  $2 \text{vol}(\Delta)$  natural choices of a directed subquiver  $\Gamma^\rightarrow$  of  $\Gamma$ , all of which are derived-equivalent.*
4. *The derived category of coherent sheaves on  $X_\Delta$  is equivalent as a triangulated category to the derived category of finitely-generated modules over the path algebra of the directed subquiver;*

$$D^b \text{coh } X_\Delta \cong D^b \text{mod } \mathbb{C}\Gamma^\rightarrow.$$

5. *The derived category of the directed Fukaya category of  $W$  is equivalent as a triangulated category to  $D^b \text{mod } \mathbb{C}\Gamma^\rightarrow$ ;*

$$D^b \mathfrak{Fuk}^\rightarrow W \cong D^b \text{mod } \mathbb{C}\Gamma^\rightarrow.$$

Here,  $\text{vol}(\Delta)$  is the Euclidean volume of  $\Delta \subset \mathbb{R}^2$ . The above theorem extends the results of [39, 40] where brane tilings for triangles and parallelograms are considered. The relation between brane tilings and vanishing cycles has also been studied by Jung and van Straten [23] in many cases including all the reflexive polygons.

The equivalence

$$D^b \text{coh } X_\Delta \cong D^b \mathfrak{Fuk}^\rightarrow W$$

obtained as the corollary of the above theorem is homological mirror symmetry for toric del Pezzo surfaces, proved by Seidel [36] for  $\mathbb{P}^2$  and  $\mathbb{P}^1 \times \mathbb{P}^1$ , Auroux, Katzarkov and Orlov [3] for Hirzebruch surfaces and Ueda [38] for

$\mathbb{P}^2$  blown-up at two or three points. Moreover, the same reasoning as in [40, section 6] proves homological mirror symmetry also for the orbifolds of toric del Pezzo surfaces by finite subgroups of the torus. See also Auroux, Katzarkov and Orlov [4] for homological mirror symmetry for del Pezzo surfaces, Abouzaid [1, 2] for an application of tropical geometry to homological mirror symmetry, and Kerr [25] for the behavior of homological mirror symmetry under weighted blowup of toric surfaces.

**Acknowledgment:** K. U. thanks Alastair Craw for invaluable discussions and explanations. M. Y. thanks Korea Institute for Advanced Study for hospitality during the final stages of this work. K. U. is supported by the 21st Century COE Program of Osaka University and Grant-in-Aid for Young Scientists (No.18840029).

## 2 Brane tilings and quivers from lattice polygons

Here we propose a mathematical formulation of the algorithm of Hanany and Vegh [22]. Let  $T = \mathbb{R}^2/\mathbb{Z}^2$  be a real two-torus equipped with an orientation. A *bipartite graph* on  $T$  consists of

- a set  $B \subset T$  of black vertices,
- a set  $W \subset T$  of white vertices, and
- a set  $E$  of edges, consisting of embedded intervals  $e$  on  $T$  such that one boundary of  $e$  belongs to  $B$  and the other boundary belongs to  $W$ . We assume that two edges intersect only at the boundaries.

A *quiver* consists of

- a set  $V$  of vertices,
- a set  $A$  of arrows, and
- two maps  $s, t : A \rightarrow V$  from  $A$  to  $V$ .

For an arrow  $a \in A$ ,  $s(a)$  and  $t(a)$  are said to be the *source* and the *target* of  $a$  respectively. A *path* on a quiver is an ordered set of arrows  $(a_n, a_{n-1}, \dots, a_1)$  such that  $s(a_{i+1}) = t(a_i)$  for  $i = 1, \dots, n-1$ . We also allow for a path of length zero, starting and ending at the same vertex. The *path algebra*  $\mathbb{C}Q$  of

a quiver  $Q = (V, A, s, t)$  is the algebra spanned by the set of paths as a vector space, and the multiplication is defined by the concatenation of paths;

$$(b_m, \dots, b_1) \cdot (a_n, \dots, a_1) = \begin{cases} (b_m, \dots, b_1, a_n, \dots, a_1) & s(b_1) = t(a_n), \\ 0 & \text{otherwise.} \end{cases}$$

A *quiver with relations* is a pair of a quiver and a two-sided ideal  $\mathcal{I}$  of its path algebra. For a quiver  $\Gamma = (Q, \mathcal{I})$  with relations, its path algebra  $\mathbb{C}\Gamma$  is defined as the quotient algebra  $\mathbb{C}Q/\mathcal{I}$ .

For a choice of an order  $<$  on the set  $V$  of vertices, the *directed subquiver*  $Q^\rightarrow$  is obtained from  $Q$  by eliminating the arrows  $a \in A$  satisfying  $s(a) > t(a)$ . The path algebra  $\mathbb{C}Q^\rightarrow$  is a subalgebra of  $\mathbb{C}Q$ , and an ideal  $\mathcal{I}$  of  $\mathbb{C}Q$  induces an ideal  $\mathcal{I}^\rightarrow = \mathcal{I} \cap \mathbb{C}Q^\rightarrow$  of  $\mathbb{C}Q^\rightarrow$ .

We are going to deal only with an ideal of relations generated by a *potential*. A potential is a formal sum of oriented cycles on the quiver, and the relations are generated by the derivatives of the potential: Let  $p = (a_n, \dots, a_1)$  be an oriented cycle on the quiver, i.e., a path such that  $s(a_1) = t(a_n)$ . For an arrow  $b$ , the *derivative* of  $p$  by  $b$  is defined by

$$\frac{\partial p}{\partial b} = \sum_{i=1}^n \delta_{a_i, b}(a_{i-1}, a_{i-2}, \dots, a_1, a_n, a_{n-1}, \dots, a_{i+1}),$$

where

$$\delta_{a,b} = \begin{cases} 1 & a = b, \\ 0 & \text{otherwise.} \end{cases}$$

This derivation extends to formal sums of oriented cycles by linearity. Let  $\Phi$  be a formal sum of oriented cycles. Then  $\Phi$  defines an ideal  $\mathcal{I} = (\partial\Phi)$  generated by the derivatives  $\partial\Phi/\partial a$  for all the arrows  $a$  of the quiver;

$$(\partial\Phi) = \left( \frac{\partial\Phi}{\partial a} \right)_{a \in A}.$$

$\Phi$  is also called *superpotential* by physicists in the context of  $\mathcal{N} = 1$  supersymmetric gauge theory in four dimension.

The most basic example is the quiver with  $V = \{v\}$  and  $A = \{x, y, z\}$ . Since there is only one vertex, the maps  $s$  and  $t$  must be constant. Consider the potential

$$\Phi = xyz - yxz.$$

The corresponding ideal is given by

$$\begin{aligned} (\partial\Phi) &= \left( \frac{\partial\Phi}{\partial x}, \frac{\partial\Phi}{\partial y}, \frac{\partial\Phi}{\partial z} \right) \\ &= (yz - zy, zx - xz, xy - yx). \end{aligned}$$

The resulting path algebra with relations is just the polynomial ring in three variables;

$$\mathbb{C}\langle x, y, z \rangle / (\partial\Phi) \cong \mathbb{C}[x, y, z].$$

See Ginzburg [18] and references therein for more on algebras whose ideals of relations are generated by potentials.

Now let us formulate the algorithm of Hanany and Vegh. Let  $\Delta \subset \mathbb{R}^2$  be a lattice polygon, i.e., the convex hull of a finite subset of  $\mathbb{Z}^2$ . An *edge* of  $\Delta$  is a connected component of the boundary  $\partial\Delta \setminus (\partial\Delta \cap \mathbb{Z}^2)$  of  $\Delta$  minus its lattice points. For example, the convex hull  $\Delta_2$  of  $(-1, 0)$ ,  $(1, 0)$  and  $(0, 1)$  shown in Figure 1 has four edges.

For an edge  $a$  of  $\Delta$ , draw an oriented line  $L_a$  on  $T$  in the direction of its primitive outward normal vector. The choice of  $L_a$  is unique only up to translations. We assume that no three lines meet at one point. The family  $\{L_a\}_a$  divides  $T$  into a finite number of polygons  $\{P_i\}_{i=1}^m$ . A polygon  $P_i$  is called *white* if the orientations of  $L_a \cap P_i$  induced from those of  $L_a$  and  $P_i$  coincides for all the edges  $a$ , and *black* if they are opposite for all the edges. A connected component of  $(\cup_a L_a) \setminus (\cup_{a,b} (L_a \cap L_b))$  can bound at most one colored polygon, and the family  $\{L_a\}_a$  is called *admissible* if it always does.

As an example, consider configurations of oriented lines coming from the triangle  $\Delta_2$  in Figure 1. There are two combinatorially distinct ways shown in Figure 2 and Figure 3 to arrange four lines in the directions of outward normal vectors of the edges of  $\Delta_2$ . In Figure 2, all the connected components of  $(\cup_a L_a) \setminus (\cup_{a,b} (L_a \cap L_b))$  bound colored polygons, whereas in Figure 3, the connected components of  $(\cup_a L_a) \setminus (\cup_{a,b} (L_a \cap L_b))$  drawn in dotted lines do not bound any colored polygon. Hence the polygon  $\Delta_2$  in Figure 1 has a unique admissible configuration.

With an admissible configuration  $\{L_a\}_a$ , one associates a bipartite graph on  $T$  called the *brane tiling* as follows; the set  $W$  of white vertices is the set of the centers of gravities of white polygons, and the set  $B$  of black vertices is the set of the centers of gravities of black polygons. For a pair of colored polygons sharing a vertex, their centers of gravities are connected by a straight line segment.

A brane tiling  $(B, W, E)$  encodes the information of a quiver  $(V, A, s, t, (\partial\Phi))$  with relations in the following way: The set  $V$  of vertices is the set of connected components of the complement  $T \setminus (\cup_{e \in E} e)$ , and the set  $A$  of arrows is the set  $E$  of edges of the graph. The directions of the arrows are determined by the colors of the vertices of the graph, so that the white vertex  $w \in W$  is on the right of the arrow. In other words, the quiver is the dual graph of the brane tiling equipped with an orientation given by rotating the white-to-black flow on the edges of the brane tiling by minus 90 degrees.

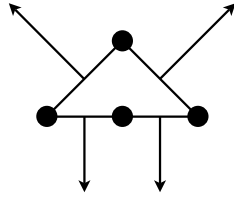


Figure 1: A triangle  $\Delta_2$

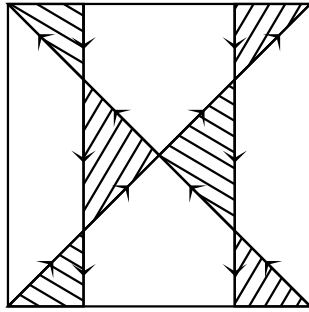


Figure 2: The admissible configuration

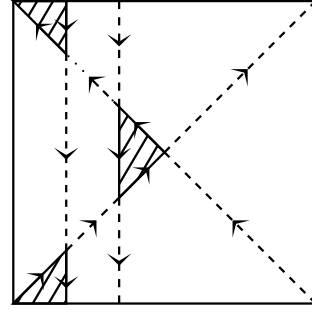


Figure 3: The non-admissible configuration

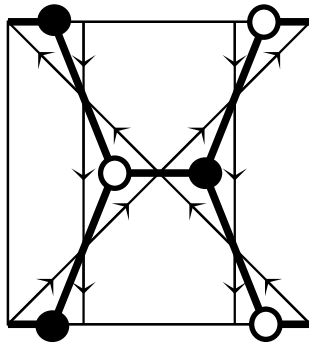


Figure 4: The brane tiling

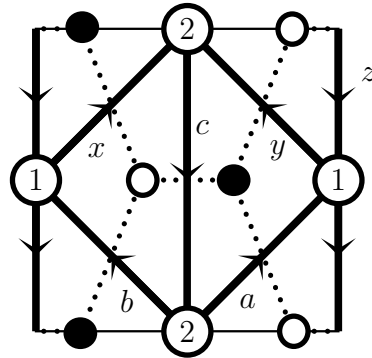


Figure 5: The quiver

The potential  $\Phi$  is defined by

$$\Phi = \sum_{w \in W} c(w) - \sum_{b \in B} c(b)$$

where  $c(w)$  is the oriented cycle encircling  $w$  clockwise and  $c(b)$  is the oriented cycle encircling  $b$  counterclockwise. The relations  $\mathcal{I} = (\partial\Phi)$  generated by the potential  $\Phi$  can be described as follows: For an arrow  $a \in A$ , there exist two paths  $p_+(a)$  and  $p_-(a)$  from  $t(a)$  to  $s(a)$ , the former going around the white vertex connected to  $a$  clockwise and the latter going around the black vertex connected to  $a$  counterclockwise. Then the ideal  $\mathcal{I}$  of the path algebra is generated by  $p_+(a) - p_-(a)$  for all  $a \in A$ .

As an example, Figure 4 shows the brane tiling associated with the admissible configuration in Figure 2, and Figure 5 shows the resulting quiver. The potential for the relations in this case is given by

$$\Phi = cxb - cya + yza - xzb.$$

### 3 Coamoebas and Newton polygons

Here we discuss the relation between the Newton polygons and asymptotic behaviors of the coamoebas. The *coamoeba* of an algebraic subvariety of a torus  $(\mathbb{C}^\times)^n$  is defined by Passare and Tsikh as its image by the argument map

$$\begin{aligned} (\mathbb{C}^\times)^n &\rightarrow (\mathbb{R}/\mathbb{Z})^n \\ \Psi &\quad \quad \quad \Psi \\ (x_1, \dots, x_n) &\mapsto \frac{1}{2\pi}(\arg(x_1), \dots, \arg(x_n)). \end{aligned} \tag{2}$$

Here  $n$  is a natural number. We consider the case when  $n = 2$ . For a Laurent polynomial

$$W(x, y) = \sum_{(i,j) \in \mathbb{Z}^2} a_{ij} x^i y^j$$

in two variables, its *Newton polygon* is defined as the convex hull of  $(i, j) \in \mathbb{Z}^2$  such that  $a_{ij} \neq 0$ ;

$$\Delta = \text{Conv}\{(i, j) \in \mathbb{Z}^2 \mid a_{ij} \neq 0\} \subset \mathbb{R}^2.$$

For an edge  $e$  of  $\Delta$ , let  $(n(e), m(e)) \in \mathbb{Z}^2$  be the primitive outward normal vector of  $e$  and  $l(e)$  be the integer such that the defining equation for the edge  $e$  is given by

$$n(e)i + m(e)j = l(e).$$

The *leading term* of  $W$  with respect to the edge  $e$  is defined by

$$W_e(x, y) = \sum_{n(e)i+m(e)j=l(e)} a_{ij}x^i y^j.$$

This is indeed the leading term if we put

$$(x, y) = (r^{n(e)}u, r^{m(e)}v), \quad r \in \mathbb{R} \text{ and } u, v \in \mathbb{C}^\times$$

and take the  $r \rightarrow \infty$  limit;

$$P(r^{n(e)}u, r^{m(e)}v) = r^{l(e)}W_e(u, v) + O(r^{l(e)-1}).$$

Now assume that for an edge  $e$ , the leading term  $W_e(x, y)$  is a binomial

$$W_e(x, y) = a_1 x^{i_1} y^{j_1} + a_2 x^{i_2} y^{j_2},$$

where  $a_1, a_2 \in \mathbb{C}$  and  $(i_1, j_1), (i_2, j_2) \in \mathbb{Z}^2$ . We can make this assumption for the purpose of this paper since the directed Fukaya category  $\mathfrak{Fuk}^\rightarrow W$  defined in section 5 does not depend on the choice of sufficiently general  $W$ . Put  $\alpha_i = \arg(a_i)$  for  $i = 1, 2$  and

$$(x, y) = (r^{n(e)}|a_2|\mathbf{e}(\theta), r^{m(e)}|a_1|\mathbf{e}(\phi)),$$

where  $\mathbf{e}(x) = \exp(2\pi\sqrt{-1}x)$  for  $x \in \mathbb{R}/\mathbb{Z}$ . Then the leading behavior of  $W$  as  $r \rightarrow \infty$  is given by

$$r^{l(e)}W_e(\mathbf{e}(\theta), \mathbf{e}(\phi)) = r^{l(e)}|a_1 a_2| \{ \mathbf{e}(\alpha_1 + i_1\theta + j_1\phi) + \mathbf{e}(\alpha_2 + i_2\theta + j_2\phi) \}. \quad (3)$$

Hence the coamoeba of  $W^{-1}(0)$  asymptotes in this limit to the line

$$(\alpha_2 - \alpha_1) + (i_2 - i_1)\theta + (j_2 - j_1)\phi + \frac{1}{2} = 0 \pmod{\mathbb{Z}}$$

on the torus  $T = (\mathbb{R}/\mathbb{Z})^2$ . This line will be called an *asymptotic boundary* of the coamoeba of  $W^{-1}(0)$ .

The asymptotic boundary has a natural orientation coming from the outward normal vector of the edge of  $\Delta$ . To understand the role of this orientation, take a pair of adjacent edges  $e$  and  $e'$  of  $\Delta$  as in Figure 6 and consider the behavior of the coamoeba of  $W^{-1}(0)$  near the intersection of asymptotic boundaries corresponding to  $e$  and  $e'$ . Assume that the leading terms corresponding to  $e$  and  $e'$  are binomials

$$\begin{aligned} W_e(x, y) &= \mathbf{e}(\alpha)x^{i_1}y^{j_1} + \mathbf{e}(\beta)x^{i_2}y^{j_2}, \\ W_{e'}(x, y) &= \mathbf{e}(\beta)x^{i_2}y^{j_2} + \mathbf{e}(\gamma)x^{i_3}y^{j_3} \end{aligned}$$

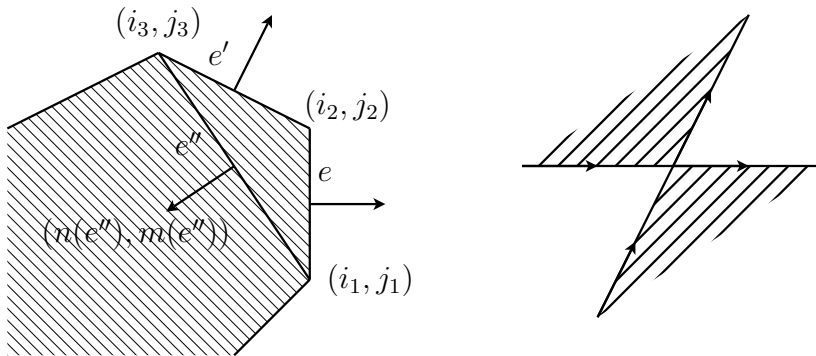


Figure 6: A pair of adjacent edges of the Newton polygon  
 Figure 7: The leading behavior of the coamoeba near an intersection of asymptotic boundaries.

for some  $\alpha, \beta, \gamma \in \mathbb{R}/\mathbb{Z}$  and  $(i_1, j_1), (i_2, j_2), (i_3, j_3) \in \mathbb{Z}^2$ . Put

$$W_{ee'}(x, y) = \mathbf{e}(\alpha)x^{i_1}y^{j_1} + \mathbf{e}(\beta)x^{i_2}y^{j_2} + \mathbf{e}(\gamma)x^{i_3}y^{j_3}.$$

Assume further that all the coefficients of  $W$  corresponding to interior lattice points of the Newton polygon of  $W_{ee'}$  vanish. Then  $W_{ee'}$  is the sum of the leading term and the subleading term of  $W$  as one puts

$$(x, y) = (r^{-n(e'')}u, r^{-m(e'')}v), \quad r \in \mathbb{R}^{>0} \text{ and } u, v \in \mathbb{C}^\times,$$

and take the  $r \rightarrow \infty$  limit. Here,  $(n(e''), m(e'')) \in \mathbb{Z}^2$  is the primitive outward normal vector of the edge  $e''$  of the Newton polygon of  $W_{ee'}$  shown in Figure 6. The coamoeba for the sum of three monomials has been analyzed in [39]; the asymptotic boundaries coincide with the actual boundaries of the coamoeba, and the orientations on the asymptotic boundaries determine which side of the boundary belongs to the coamoeba. Hence the orientations of asymptotic boundaries determine the leading behavior of the coamoeba near the intersections of asymptotic boundaries as in Figure 7.

## 4 Perfect matchings and line bundles

Here we recall definitions from the dimer theory and explain the method of Hanany, Herzog and Vegh [20] to produce collections of line bundles on toric Fano surfaces from brane tilings. Let  $G = (B, W, E)$  be a brane tiling on the torus  $T = \mathbb{R}^2/\mathbb{Z}^2$  and  $(V, A, s, t, \mathcal{I})$  be the corresponding quiver with relations. A *perfect matching* (or a *dimer configuration*) of  $G$  is a subset  $D$  of  $E$  such that for any vertex  $v \in B \cup W$ , there is a unique edge  $e \in D$  connected to  $v$ . Consider the bipartite graph  $\tilde{G}$  on  $\mathbb{R}^2$  obtained from  $G$

by pulling-back by the natural projection  $\mathbb{R}^2 \rightarrow T$ , and identify the set of perfect matchings of  $G$  with the set of periodic perfect matchings of  $\tilde{G}$ . Fix a reference perfect matching  $D_0$ . Then for any perfect matching  $D$ , the union  $D \cup D_0$  divides  $\mathbb{R}^2$  into connected components. The height function  $h_{D,D_0}$  is a locally-constant function on  $\mathbb{R}^2 \setminus (D \cup D_0)$  which increases (resp. decreases) by 1 when one crosses an edge  $e \in D$  with the black (resp. white) vertex on his right or an edge  $e \in D_0$  with the white (resp. black) vertex on his right. This rule determines the height function up to additions of constants. The height function may not be periodic even if  $D$  and  $D_0$  are periodic, and the *height change*  $h(D, D_0) = (h_x(D, D_0), h_y(D, D_0)) \in \mathbb{Z}^2$  of  $D$  with respect to  $D_0$  is defined as the difference

$$\begin{aligned} h_x(D, D_0) &= h_{D,D_0}(p + (1, 0)) - h_{D,D_0}(p), \\ h_y(D, D_0) &= h_{D,D_0}(p + (0, 1)) - h_{D,D_0}(p) \end{aligned}$$

of the height function, which does not depend on the choice of  $p \in \mathbb{R}^2 \setminus (D \cup D_0)$ . The dependence of the height change on the choice of the reference matching is given by

$$h(D, D_1) = h(D, D_0) - h(D_1, D_0)$$

for any three perfect matchings  $D$ ,  $D_0$  and  $D_1$ . We will often suppress the dependence of the height difference on the reference matching and just write  $h(D) = h(D, D_0)$ .

The *characteristic polynomial*  $K(x, y) \in \mathbb{C}[x^{\pm 1}, y^{\pm 1}]$  of the bipartite graph with respect to a reference matching  $D_0$  is defined as the sum

$$K(x, y) = \sum_D (-1)^{h_x(D)h_y(D)+h_x(D)+h_y(D)} x^{h_x(D)} y^{h_y(D)}$$

over the set of perfect matchings. The absolute values of the coefficients of the characteristic polynomial are called *multiplicities* of the height changes. By taking the Newton polygon of  $K(x, y)$ , one obtains a lattice polygon. If one changes the choice of a reference matching, the Newton polygon will be translated.

As an example, consider the bipartite graph in Figure 8 appearing in [39, Figure 7]. This graph has six perfect matchings  $D_i$ ,  $i = 1, \dots, 6$  shown in Figures 9–14. Figure 15 shows the height function of  $D_1$  with  $D_4$  as a reference matching. The captions on Figures 9–14 show the height changes with  $D_4$  as a reference matching. The characteristic polynomial of this graph is

$$K(x, y) = -x - y - \frac{1}{xy} + 3. \tag{4}$$

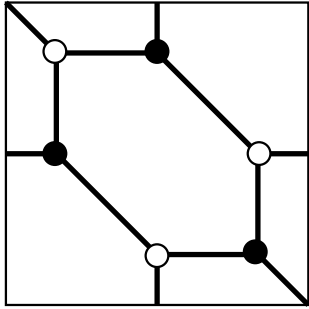


Figure 8: A bipartite graph

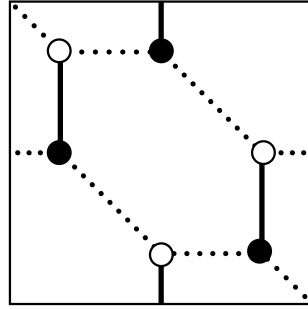


Figure 9:  $D_1 : (1, 0)$

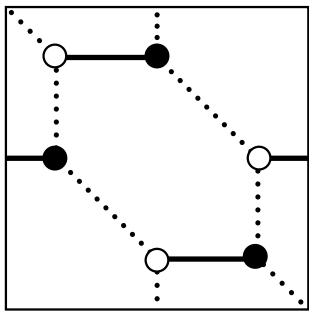


Figure 10:  $D_2 : (0, 1)$

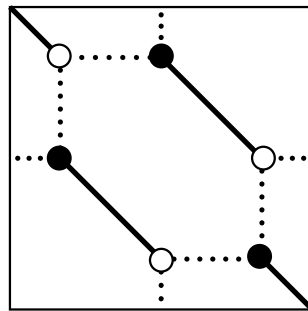


Figure 11:  $D_3 : (-1, -1)$

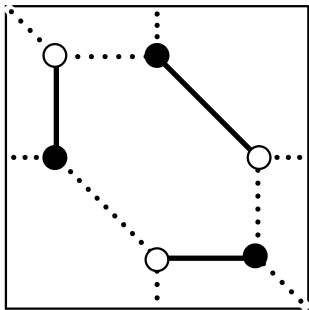


Figure 12:  $D_4 : (0, 0)$

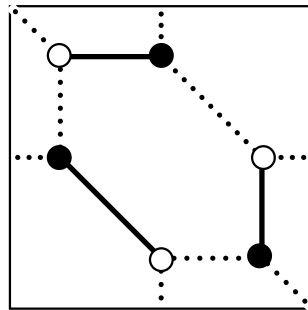


Figure 13:  $D_5 : (0, 0)$

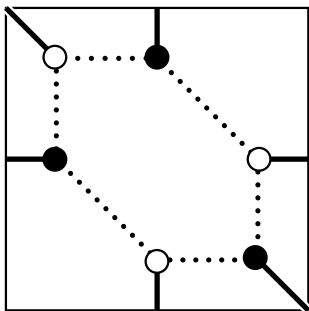


Figure 14:  $D_6 : (0, 0)$

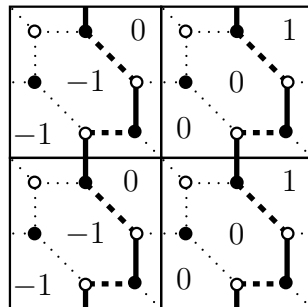


Figure 15: The height function for  $D_1$  with respect to  $D_4$

To a perfect matching  $D$ , one can associate a subquiver of  $(V, A, s, t)$  by eliminating the arrows which cross edges in  $D$ . As an example, Figure 16 and Figure 17 show the subquivers corresponding to the perfect matchings  $D_1$  and  $D_4$  respectively. Note that the subquivers corresponding to  $D_4, D_5$  and  $D_6$  are the directed subquivers with respect to choices of orders on the set of vertices, whereas the subquivers corresponding to  $D_1, D_2$  and  $D_3$  are not. Note further that the cyclic orderings on the set of vertices induced by the matchings  $D_4, D_5$ , and  $D_6$  coincide.

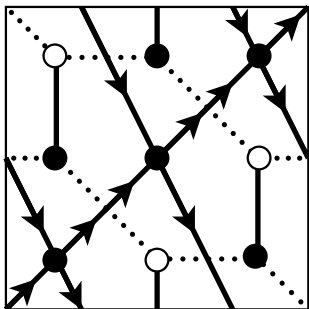


Figure 16: The subquiver for  $D_1$

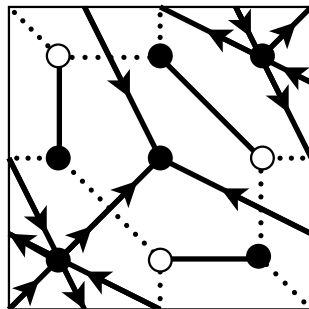


Figure 17: The subquiver for  $D_4$

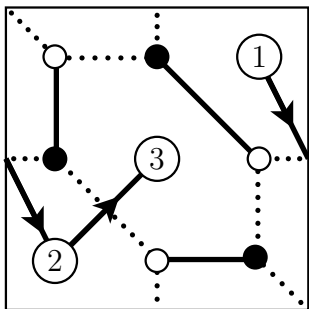


Figure 18: A path on the subquiver for  $D_4$

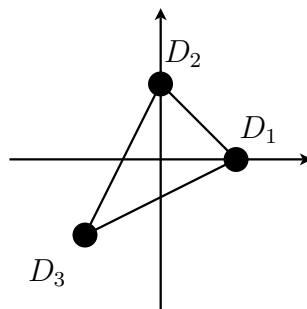


Figure 19: The Newton polygon  $\Delta_3$

An *internal* matching is a perfect matching  $D$  whose height change  $(h_x, h_y)$  lies in the interior of the Newton polygon of the characteristic polynomial  $K(x, y)$ . A perfect matching which corresponds to the vertex of the Newton polygon will be called a *vertex matching*.

In the above example, the perfect matchings  $D_1, D_2$  and  $D_3$  are vertex, whereas  $D_4, D_5$  and  $D_6$  are internal. In general, there may exist a matching which is neither internal nor vertex.

Given an internal perfect matching  $D$  of a brane tiling  $G$ , one can consider the toric stack  $X_D$  associated with the Newton polygon  $\Delta_D$  of the characteristic polynomial of  $G$  with  $D$  as a reference matching. In this situation, Hanany, Herzog and Vegh [20] proposed the following method to produce

a collection of line bundles on  $X_D$ , which conjecturally gives a full strong exceptional collection whose total morphism algebra is isomorphic to the path algebra of the subquiver with relations corresponding to  $D$ : Assume that all the vertices of  $\Delta_D$  have multiplicity one, so that the set of vertex matchings of  $G$  can be identified with the set of toric divisors on  $X_D$ . For a vertex matching  $E$ , the corresponding toric divisor will be denoted by  $D_E$ . Fix an internal matching  $D$  and assume that the corresponding subquiver is the directed subquiver for a choice of an order on the set of vertices of the quiver. Let  $N$  be the number of vertices of the quiver. Assume further that there exists a path on the subquiver which passes through all the vertices. Fix such a path. For a vertex matching  $E$  and  $1 \leq i \leq N$ , let  $a_{i,E}$  be the number of edges in  $E$  crossed by the path from the first to the  $i$ -th vertex. Then the  $i$ -th line bundle in the collection will be given by  $\mathcal{O}(\sum_E a_{i,E} D_E)$  where the sum is over the set of vertex matchings. The linear equivalence class of  $\sum_E a_{i,E} D_E$  does not depend on the choice of a path on the directed subquiver, although the divisor  $\sum a_{i,E} D_E$  itself does [20].

As an example, consider the internal matching  $D_4$  in Figure 12 and take the path in Figure 18. The Newton polygon  $\Delta_3$  of the characteristic polynomial (4) is shown in Figure 19, and the corresponding toric surface is the projective plane  $\mathbb{P}^2$ . The method of Hanany, Herzog and Vegh gives

$$\begin{aligned} \sum a_{1,E} D_E &= 0, \\ \sum a_{2,E} D_E &= 0 \cdot D_1 + 1 \cdot D_2 + 0 \cdot D_3, \\ \sum a_{3,E} D_E &= 0 \cdot D_1 + 1 \cdot D_2 + 1 \cdot D_3, \end{aligned}$$

and hence the full strong exceptional collection  $(\mathcal{O}_{\mathbb{P}^2}, \mathcal{O}_{\mathbb{P}^2}(1), \mathcal{O}_{\mathbb{P}^2}(2))$  on  $\mathbb{P}^2$  given by Beilinson [5].

## 5 Fukaya category

Here we recall the definition of the directed Fukaya category, defined by Seidel [35] following an idea of Kontsevich [27]. First we recall the definition of an  $A_\infty$ -category. For a  $\mathbb{Z}$ -graded vector space  $N = \bigoplus_{j \in \mathbb{Z}} N^j$  and an integer  $i$ , the  $i$ -th shift of  $N$  to the left will be denoted by  $N[i]$ ;  $(N[i])^j = N^{i+j}$ .

**Definition 2.** An  $A_\infty$ -category  $\mathcal{A}$  consists of

- the set  $\mathfrak{Ob}(\mathcal{A})$  of objects,
- for  $c_1, c_2 \in \mathfrak{Ob}(\mathcal{A})$ , a  $\mathbb{Z}$ -graded vector space  $\text{hom}_{\mathcal{A}}(c_1, c_2)$  called the space of morphisms, and

- operations

$$\mathbf{m}_l : \text{hom}_{\mathcal{A}}(c_{l-1}, c_l)[1] \otimes \cdots \otimes \text{hom}_{\mathcal{A}}(c_0, c_1)[1] \longrightarrow \text{hom}_{\mathcal{A}}(c_0, c_l)[1]$$

of degree  $+1$  for  $l = 1, 2, \dots$  and  $c_i \in \mathfrak{Ob}(\mathcal{A})$ ,  $i = 0, \dots, l$ , satisfying the  $A_\infty$ -relations

$$\sum_{i=0}^{l-1} \sum_{j=i+1}^l (-1)^{\deg a_1 + \cdots + \deg a_i} \mathbf{m}_{l+i-j+1}(a_l \otimes \cdots \otimes a_{j+1} \otimes \mathbf{m}_{j-i}(a_j \otimes \cdots \otimes a_{i+1}) \otimes a_i \otimes \cdots \otimes a_1) = 0, \quad (5)$$

for any positive integer  $l$ , any sequence  $c_0, \dots, c_l$  of objects of  $\mathcal{A}$ , and any sequence of morphisms  $a_i \in \text{hom}_{\mathcal{A}}(c_{i-1}, c_i)$  for  $i = 1, \dots, l$ . Here, degrees are counted after shifts; if  $a_i \in \text{hom}_{\mathcal{A}}^p(c_{i-1}, c_i)$ , then  $\deg a_i = p - 1$  in  $\text{hom}_{\mathcal{A}}(c_{i-1}, c_i)[1]$ .

Since the  $A_\infty$ -relation (5) for  $l = 1$  ensures that  $\mathbf{m}_1$  squares to zero, we can define the *cohomology category*  $H^0(\mathcal{A})$  of an  $A_\infty$ -category  $\mathcal{A}$  by  $\mathfrak{Ob}(H^0(\mathcal{A})) = \mathfrak{Ob}(\mathcal{A})$  and  $\text{hom}_{H^0(\mathcal{A})}(c_0, c_1) = H^0(\text{hom}_{\mathcal{A}}(c_0, c_1), \mathbf{m}_1)$ .

An example of an  $A_\infty$ -category comes from a *differential graded category*, i.e., a category whose spaces of morphisms are complexes such that the differential  $d$  satisfies the Leibniz rule with respect to the composition  $\circ$ ;

$$d(x \circ y) = (dx) \circ y + (-1)^{\deg x} x \circ (dy).$$

It gives rise to an  $A_\infty$ -category by

$$\begin{aligned} \mathbf{m}_1(x) &= (-1)^{\deg x} dx, \\ \mathbf{m}_2(x, y) &= (-1)^{(\deg x + 1) \deg y} x \circ y, \\ \mathbf{m}_k &= 0 \quad \text{for } k \geq 3. \end{aligned}$$

To define the derived category of an  $A_\infty$ -category, we need the concept of *twisted complexes*. It is originally due to Bondal and Kapranov [7] in the case of differential graded categories (i.e., when  $\mathbf{m}_k = 0$  for  $k \geq 3$ ), and generalized to  $A_\infty$ -categories by Kontsevich [26]. The following definition is taken from Seidel [37, section 2].

**Definition 3.** Let  $\mathcal{A}$  be an  $A_\infty$ -category.

1. The *additive enlargement*  $\Sigma\mathcal{A}$  is obtained from  $\mathcal{A}$  by formally adding direct sums and shifts; an object  $c$  of  $\Sigma\mathcal{A}$  is a formal sum

$$c = \bigoplus_{i \in I} c_i[l_i]$$

where  $I$  is a finite index set,  $c_i \in \mathfrak{Ob}(\mathcal{A})$ , and  $l_i \in \mathbb{Z}$ . The space of morphisms is given by

$$\mathrm{hom}_{\Sigma\mathcal{A}} \left( \bigoplus_{i \in I} c_i[l_i], \bigoplus_{j \in J} d_j[m_j] \right) = \bigoplus_{i,j} \mathrm{hom}_{\mathcal{A}}(c_i, d_j)[m_j - l_i].$$

$A_\infty$ -operations are inherited from those of  $\mathcal{A}$  with the following extra signs; for  $a_1 \in \mathrm{hom}_{\mathcal{A}}(c_0[l_0], c_1[l_1]), \dots, a_k \in \mathrm{hom}_{\mathcal{A}}(c_{k-1}[l_{k-1}], c_k[l_k])$ ,

$$\mathbf{m}_k^{\Sigma\mathcal{A}}(a_k, \dots, a_1) = (-1)^{l_0} \mathbf{m}_k^{\mathcal{A}}(a_k, \dots, a_1).$$

2. A *twisted complex* over  $\mathcal{A}$  is a set  $(\{c_i\}_{i \in I}, \{x_{ij}\}_{i,j \in I})$ , where  $I \subset \mathbb{Z}$  is a finite index set,  $c_i$  is an object of  $\Sigma\mathcal{A}$ , and  $x_{ij}$  is an element of  $\mathrm{hom}_{\Sigma\mathcal{A}}^{i-j+1}(c_i, c_j)$  satisfying

$$\sum_{n=1}^{\infty} \sum_{l=l_0 < l_1 < \dots < l_n=m} \mathbf{m}_n(x_{l_{n-1}l_n} \otimes \dots \otimes x_{l_0l_1}) = 0$$

for any  $l, m \in \mathbb{Z}$ . We assume  $x_{ij} = 0$  for  $i > j$ .

Twisted complexes form an  $A_\infty$ -category:

**Lemma 4.** *For an  $A_\infty$ -category  $\mathcal{A}$ , there is another  $A_\infty$ -category  $\mathrm{Pre}\text{-}\mathrm{Tr}(\mathcal{A})$  whose objects are twisted complexes of  $\mathcal{A}$  such that the space of morphisms between two twisted complexes  $c = (\{c_i\}_i, \{x_{ij}\}_{i,j})$  and  $d = (\{d_i\}_i, \{y_{ij}\}_{i,j})$  is*

$$\bigoplus_{i,j} \mathrm{hom}_{\Sigma\mathcal{A}}(c_i[-i], d_j[-j]).$$

See e.g. [16] for an explicit formula of the  $A_\infty$ -operations and the proof of the  $A_\infty$ -relations. The cohomology category of  $\mathrm{Pre}\text{-}\mathrm{Tr}(\mathcal{A})$  is called the *bounded derived category* of  $\mathcal{A}$  and will be denoted by  $D^b(\mathcal{A})$ . It has a natural structure of a triangulated category by a straightforward adaptation of [7, Proposition 2] to the  $A_\infty$  situation.

Now we recall the definition of the directed Fukaya category introduced by Seidel [35]. A Kähler manifold  $M$  is called *exact* if there is a one-form  $\theta$  on  $M$  such that the Kähler form  $\omega$  is given by  $\omega = d\theta$ . A holomorphic function  $W : M \rightarrow \mathbb{C}$  on an exact Kähler manifold  $M$  is called an *exact Lefschetz fibration* if all the critical values are distinct and all the critical points of  $W$  are non-degenerate, i.e., the Hessian  $\det(\partial_i \partial_j W)$  at any critical point is non-zero. If we view  $W$  as a fibration of Kähler manifolds outside the critical points, it has a natural horizontal distribution defined as the

orthogonal complement with respect to  $\omega$  of the tangent space to the fiber. This allows us to lift a smooth path  $c : [0, 1] \rightarrow \mathbb{C}$  on  $\mathbb{C}$  to a smooth path  $\tilde{c}_p : [0, 1] \rightarrow M$  on  $M$  starting from a point  $p \in W^{-1}(c(0))$ , as long as it does not intersect a critical point of  $W$ .

An ordered set  $(c_i)_{i=1}^N$  of smooth paths  $c_i : [0, 1] \rightarrow \mathbb{C}$  is called a *distinguished set of vanishing paths* if

1. the base point  $c_i(0)$  is a regular value of  $W$  independent of  $i$ ,
2.  $\{c_i(1)\}_{i=1}^N$  is the set of critical values of  $W$ ,
3.  $c_i$  has no self-intersection,
4. images of  $c_i$  and  $c_j$  intersects only at the base point,
5.  $c'_i(0) \neq 0$  for  $i = 1, \dots, N$ , and
6.  $\arg c'_{i+1}(0) < \arg c'_i(0)$ ,  $i = 1, \dots, N - 1$ , for a choice of a branch of the argument map.

Given a distinguished set  $(c_i)_{i=1}^N$  of vanishing paths, the corresponding *distinguished basis  $(C_i)_{i=1}^N$  of vanishing cycles* is defined by

$$C_i = \{p \in W^{-1}(c_i(0)) \mid \lim_{t \rightarrow 1} \tilde{c}_p(t) = p_i\}, \quad 1 \leq i \leq N.$$

They are exact Lagrangian submanifolds of  $W^{-1}(c_i(0))$ ;

$$\dim_{\mathbb{R}} C_i = \dim_{\mathbb{C}} W^{-1}(c_i(0)), \quad \omega|_{C_i} = 0, \quad \text{and} \quad [\theta|_{C_i}] = 0 \in H^1(C_i; \mathbb{R}).$$

The *directed Fukaya category*  $\mathfrak{Fuk}^{\rightarrow} W$  of an exact Lefschetz fibration  $W$  is an  $A_{\infty}$ -category whose set of objects is a distinguished basis of vanishing cycles and whose spaces of morphisms are Lagrangian intersection Floer complexes. The Lagrangian intersection Floer complex of two exact Lagrangian submanifolds is defined by Floer [11]. The  $A_{\infty}$ -structure is introduced by Fukaya [15] and used by Kontsevich [26] to formulate his *homological mirror symmetry* conjecture. The task of defining Fukaya categories in full generality is undertaken by Fukaya, Oh, Ohta and Ono [17].

In this paper, we restrict ourselves to the case when  $M$  is an algebraic torus  $(\mathbb{C}^{\times})^2 = \text{Spec } \mathbb{C}[x^{\pm 1}, y^{\pm 1}]$  equipped with the Kähler form

$$\omega = -\frac{\sqrt{-1}}{2} \left( \frac{dx \wedge d\bar{x}}{|x|^2} + \frac{dy \wedge d\bar{y}}{|y|^2} \right)$$

and  $W : (\mathbb{C}^{\times})^2 \rightarrow \mathbb{C}$  is a regular map defined by a Laurent polynomial. Assume that the origin  $0 \in \mathbb{C}$  is a regular value of  $W$  and take it as the base

point of a distinguished set of vanishing paths;  $c_i(0) = 0$  for  $1 \leq i \leq N$ . Assume further that the corresponding vanishing cycles  $C_i$  intersect each other transversally. This assumption can always be met by moving them within their Hamiltonian isotopy classes. In this situation, vanishing cycles are just curves on the Riemann surface  $W^{-1}(0)$ , and  $\mathfrak{Fuk}^{\rightarrow} W$  can be computed in a purely combinatorial way. The exposition below follows Seidel [37, section (9e)] closely:

First we discuss the grading on Floer complexes [12, 26, 34]. Let

$$\Omega = \text{Res} \frac{dx \wedge dy}{xyW(x,y)}$$

be the holomorphic 1-form on  $W^{-1}(0)$  defined as the residue of a holomorphic 2-form on  $(\mathbb{C}^\times)^2 \setminus W^{-1}(0)$ . When the origin is the only interior lattice point of the Newton polygon of  $W$  so that  $W^{-1}(0)$  is an affine elliptic curve, the above  $\Omega$  gives the restriction of the unique (up to scalar multiples) holomorphic 1-form on the completion of  $W^{-1}(0)$ . For  $1 \leq i \leq N$ , the *phase function* on the vanishing cycle  $C_i \subset W^{-1}(0)$  is defined by

$$\begin{array}{ccc} \phi_{C_i} : C_i & \rightarrow & S^1 \cong \mathbb{C}^\times / \mathbb{R}^{>0} \\ \downarrow & & \downarrow \\ p & \mapsto & [\Omega(T_p C_i)]^2. \end{array}$$

A *grading* of  $C_i$  is a lift  $\tilde{\phi}_{C_i} : C_i \rightarrow \mathbb{R}$  of  $\phi_{C_i}$  to the universal cover  $\mathbb{R}$  of  $S^1 \cong \mathbb{R}/\mathbb{Z}$ . Such a lift always exists, and one has as many as  $\mathbb{Z}$  choices for each  $i$ . Note that the grading of  $C_i$  modulo  $2\mathbb{Z}$  defines an orientation on  $C_i$ . Fix gradings on vanishing cycles  $C_1, \dots, C_N$ . For an intersection point  $p \in C_i \cap C_j$  of two vanishing cycles, the *Maslov index*  $\mu(p)$  is defined as the smallest integer greater than  $\tilde{\phi}_{C_j}(p) - \tilde{\phi}_{C_i}(p)$ ;

$$\mu(p) = \lfloor \tilde{\phi}_{C_j}(p) - \tilde{\phi}_{C_i}(p) \rfloor.$$

Next we fix *spin structures* of vanishing cycles to orient the moduli spaces of pseudoholomorphic disks with Lagrangian boundary conditions. Since vanishing cycles are just circles in our case, the choice of spin structures is equivalent to the choice of their two-fold covers. We take the non-trivial spin structures, and hence the non-trivial covers, so that they extend to the unique spin structures on the Lefschetz thimbles. We fix a branch point on each vanishing cycle where two sheets of the non-trivial cover get exchanged.

The directed Fukaya category  $\mathfrak{Fuk}^{\rightarrow} W$  is an  $A_\infty$ -category whose set of

objects is  $(C_i)_{i=1}^N$  and whose spaces of morphisms are

$$\mathrm{hom}_{\mathfrak{S}\mathrm{ut} \rightarrow W}(C_i, C_j) = \begin{cases} 0 & i > j, \\ \mathbb{C} \cdot \mathrm{id}_{C_i} & i = j, \\ \bigoplus_{p \in C_i \cap C_j} \mathrm{span}_{\mathbb{C}}\{p\} & i < j, \end{cases}$$

where  $\deg p = \mu(p)$ . For a positive integer  $k$ , a sequence  $(C_{i_0}, \dots, C_{i_k})$  of objects, and morphisms  $p_l \in C_{i_{l-1}} \cap C_{i_l}$  for  $l = 1, \dots, k$ , the  $A_\infty$ -operation  $\mathfrak{m}_k$  is given by counting with signs the number of holomorphic disks with Lagrangian boundary conditions;

$$\mathfrak{m}_k(p_k, \dots, p_1) = \sum_{p_0 \in C_{i_0} \cap C_{i_k}} \# \overline{M}_{k+1}(C_{i_0}, \dots, C_{i_k}; p_0, \dots, p_k) p_0.$$

Here,  $\overline{M}_{k+1}(C_{i_0}, \dots, C_{i_k}; p_0, \dots, p_k)$  is the moduli space of holomorphic maps  $\phi : D^2 \rightarrow W^{-1}(0)$  from the unit disk  $D^2$  with  $k+1$  marked points  $(z_0, \dots, z_k)$  on the boundary respecting the cyclic order, with the following boundary condition: Let  $\partial_l D^2 \in \partial D^2$  be the interval between  $z_l$  and  $z_{l+1}$ , where we set  $z_{k+1} = z_0$ . Then  $\phi(\partial_l D^2) \subset C_{i_l}$  and  $\phi(z_l) = p_l$  for  $l = 0, \dots, k$ . The sign for the contribution of  $\phi$  is given by  $(-1)^\dagger$ , where  $\dagger$  is the sum of (i) the number of  $1 \leq l \leq k$  such that  $(C_{i_{l-1}} \cdot C_{i_l})_{p_l} = 1$  and the orientation of  $C_{i_l}$  points away from  $\phi(D)$ , (ii) one if  $(C_{i_0} \cdot C_{i_k})_{p_0} = 1$  and the orientation of  $C_{i_0}$  points toward  $\phi(D)$ , and (iii) the number of the base points for the spin structures on  $\phi(\partial D)$ .

## 6 The brane tiling for $\mathbb{P}^2$ blown-up at one point

Let  $X_4$  be the projective plane blown-up at one point. The lattice polygon for  $X_4$  is the convex hull  $\Delta_4$  of

$$v_1 = (1, 0), v_2 = (0, 1), v_3 = (-1, 0), \text{ and } v_4 = (-1, -1)$$

as shown in Figure 20. The primitive outward normal vectors of the edges of  $\Delta_4$  are given by

$$n_1 = (1, 1), n_2 = (-1, 1), n_3 = (-1, 0), \text{ and } n_4 = (1, -2).$$

**Lemma 5.** *There is a unique admissible configuration of oriented lines corresponding to  $\Delta_4$ .*

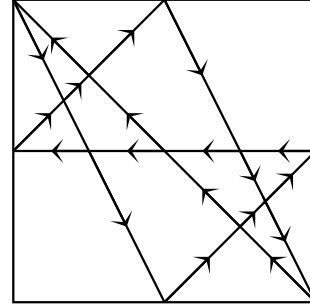
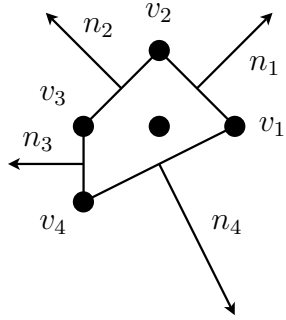


Figure 20: The lattice polygon  $\Delta_4$  with its primitive normal vectors      Figure 21: The unique admissible configuration corresponding to  $\Delta_4$

Here, the uniqueness is up to small perturbations which do not change the combinatorial structure. This unique admissible configuration is shown in Figure 21.

*Proof.* Figure 22 shows the unique configuration of three oriented lines on the torus in the directions of  $n_1, n_2$ , and  $n_4$ . There are five combinatorially distinct ways to insert a line into Figure 22 in the direction of  $n_3$  shown in Figure 23. In addition, since two of six intersection points of the three lines

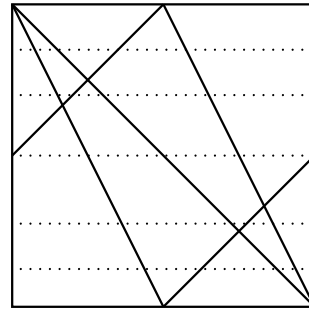
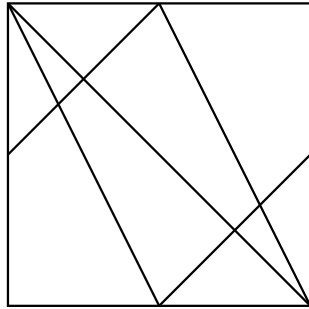


Figure 22: The unique configuration of three lines in the directions of  $n_1, n_2$  and  $n_4$       Figure 23: Five ways to insert the fourth line in the direction of  $n_3$

in Figure 22 are on the same horizontal level, there are two combinatorially distinct ways shown in Figure 24 and Figure 25 to perturb them a little and insert the fourth line. It is easy to see that only one of these seven configurations is admissible.  $\square$

Figure 26 shows the brane tiling corresponding to this unique admissible configuration of lines. The resulting quiver is shown in Figure 27. The potential  $\Phi$  generating the relation  $\mathcal{I}$  of its path algebra is given by

$$\Phi = g_2ca_1f_1 - g_1ca_2f_1 + g_1bf_2 - da_1f_2 + da_2f_3 - g_2bf_3 \quad (6)$$

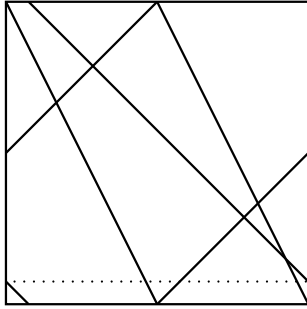


Figure 24: one way to perturb three lines to insert the fourth line

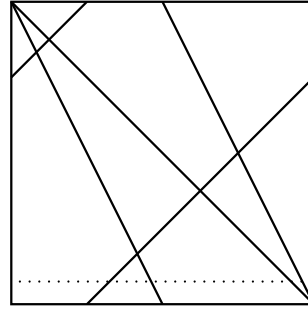


Figure 25: another way to perturb three lines to insert the fourth line

The brane tiling in Figure 26 has eight perfect matchings. Four of them are vertex as shown in Figures 28–31. The captions on these figures show the corresponding height changes. Figures 32–35 show the remaining four matchings together with the corresponding subquiver. Their height changes are  $(0, 0)$  so that they are internal matchings. On the right of Figures 32–35 are shown the corresponding subquivers. They turn out to be the directed subquivers with respect to orderings on the set of vertices. The captions on Figures 32–35 show the collections  $(E_1, \dots, E_4)$  of line bundles on  $X_4$  obtained through the algorithm of Hanany, Herzog and Vegh explained in section 4. Here,  $H$  is the strict transform of the hyperplane in  $\mathbb{P}^2$  and  $E$  is the exceptional divisor. One can see that internal matchings correspond to foundations of the strong helix

$$\dots, \mathcal{O}(E - H), \mathcal{O}, \mathcal{O}(E), \mathcal{O}(H), \mathcal{O}(2H), \mathcal{O}(3H - E), \mathcal{O}(3H), \mathcal{O}(4H - E), \dots \quad (7)$$

of period four, consisting of line bundles. See Rudakov et al.[32] for the definitions of exceptional collections and helices.

The path algebra  $\mathbb{C}\Gamma_4$  with relations of the quiver in Figure 27 is isomorphic to the rolled-up helix algebra (in the sense of Bridgeland [8, section 4.1]) of the strong helix (7). Then [8, Proposition 4.1] shows that the derived category of coherent sheaves on the total space of the canonical bundle  $K_{X_4}$  is equivalent as a triangulated category to the derived category of finitely-generated right  $\mathbb{C}\Gamma_4$ -modules;

$$D^b \text{coh } K_{X_4} \cong D^b \text{coh } \mathbb{C}\Gamma_4.$$

Let  $\Gamma_4^\rightarrow$  be one of the directed subquivers of  $\Gamma$  in Figures 32–35. Since  $\mathbb{C}\Gamma_4^\rightarrow$  is isomorphic to the total morphism algebra

$$\mathbb{C}\Gamma_4^\rightarrow \cong \bigoplus_{i,j=1}^4 \text{hom}(E_i, E_j)$$

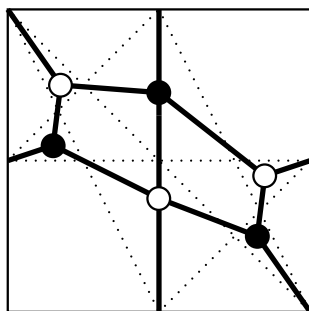


Figure 26: The brane tiling

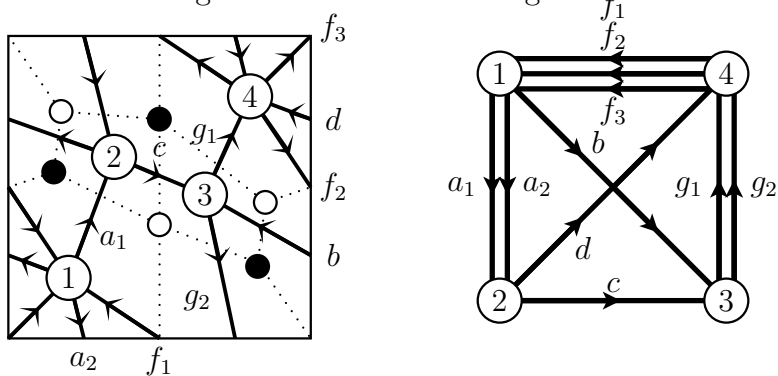


Figure 27: The quiver  $\Gamma_4$

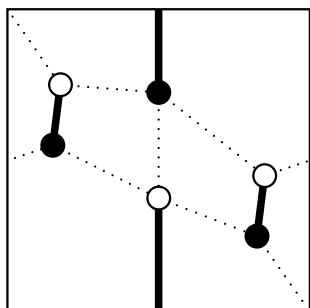


Figure 28:  $(h_x, h_y) = (1, 0)$

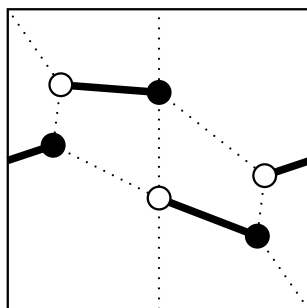


Figure 29:  $(h_x, h_y) = (0, 1)$

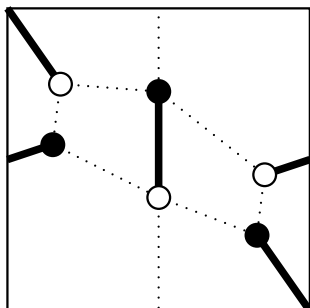


Figure 30:  $(h_x, h_y) = (-1, 0)$

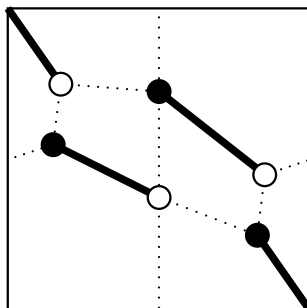


Figure 31:  $(h_x, h_y) = (-1, -1)$

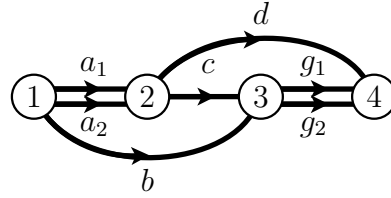
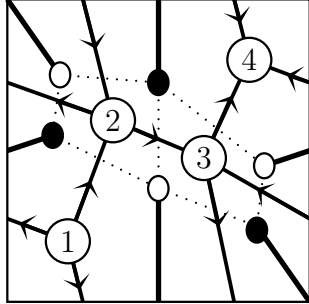


Figure 32:  $(\mathcal{O}, \mathcal{O}(H - E), \mathcal{O}(H), \mathcal{O}(2H - E))$

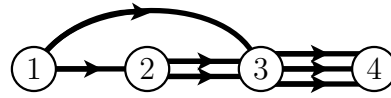
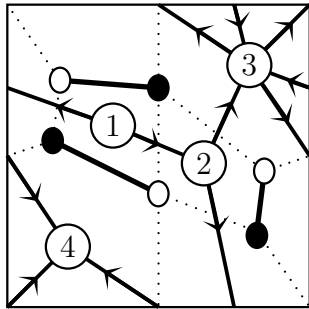


Figure 33:  $(\mathcal{O}, \mathcal{O}(E), \mathcal{O}(H), \mathcal{O}(2H))$

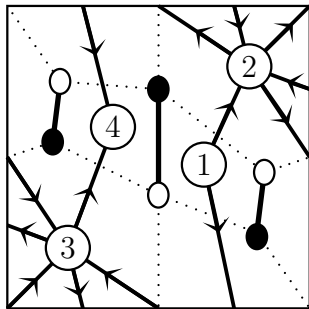


Figure 34:  $(\mathcal{O}, \mathcal{O}(H - E), \mathcal{O}(2H - E), \mathcal{O}(3H - 2E))$

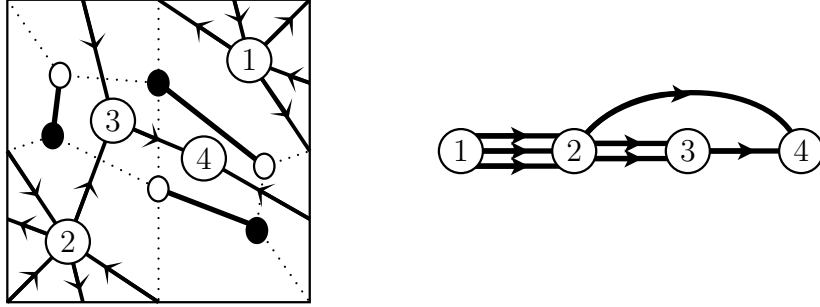


Figure 35:  $(\mathcal{O}, \mathcal{O}(H), \mathcal{O}(2H - E), \mathcal{O}(2H))$

of the full strong exceptional collection  $(E_1, \dots, E_4)$ , we have an equivalence

$$D^b \text{coh } X_4 \cong D^b \text{mod } \mathbb{C}\Gamma_4^{\rightarrow} \quad (8)$$

of triangulated categories by Bondal [6, Theorem 6.2]. Let  $P_i$  and  $S_i$  be the projective module and the simple module corresponding to the  $i$ -th vertex of the quiver  $\Gamma_4^{\rightarrow}$  for  $1 \leq i \leq 4$ . The sequence  $(P_i)_{i=1}^4$  gives a full strong exceptional collection in  $D^b \text{mod } \mathbb{C}\Gamma_4^{\rightarrow}$  whose total morphism algebra is isomorphic to  $\mathbb{C}\Gamma_4^{\rightarrow}$ , whereas the sequence  $(S_i)_{i=1}^4$  gives another full exceptional collection which is left dual to  $(P_i)_{i=1}^4$  [6, Lemma 5.6].

Let  $\mathcal{A}$  be the full subcategory of the enhancement (in the sense of Bondal–Kapranov [7]) of  $D^b \text{mod } \mathbb{C}\Gamma_4^{\rightarrow}$  consisting of  $\{S_i\}_{i=1}^4$ . Consider  $\mathcal{A}$  as an  $A_\infty$ -category and let  $D^b \mathcal{A}$  be the derived category of  $\mathcal{A}$  defined in section 5 using twisted complexes. Since  $(S_i)_{i=1}^4$  generates  $D^b \text{mod } \mathbb{C}\Gamma_4^{\rightarrow}$  as a triangulated category, one has an equivalence

$$D^b \mathcal{A} \cong D^b \text{mod } \mathbb{C}\Gamma_4^{\rightarrow}$$

by Bondal and Kapranov [7, §4, Theorem 1].

Now we construct the *minimal model* of  $\mathcal{A}$ , i.e., an  $A_\infty$ -category  $\mathcal{B}$  quasi-isomorphic to  $\mathcal{A}$  such that  $\mathfrak{m}_1^{\mathcal{B}} = 0$ . To carry out the construction explicitly, take the quiver in Figure 32 as an example. We use the projective resolutions

$$\begin{aligned} 0 &\longrightarrow P_1 \xrightarrow{\sim} S_1 \longrightarrow 0, \\ 0 &\longrightarrow \begin{array}{c} P_1^{\oplus 2} \\ \cup \\ (x, y) \end{array} \xrightarrow{\phi_2} \begin{array}{c} P_2 \\ \cup \\ a_1x + a_2y \end{array} \longrightarrow S_2 \longrightarrow 0, \\ 0 &\longrightarrow \begin{array}{c} P_1 \oplus P_2 \\ \cup \\ (x, y) \end{array} \xrightarrow{\phi_3} \begin{array}{c} P_3 \\ \cup \\ bx + cy \end{array} \longrightarrow S_3 \longrightarrow 0, \end{aligned}$$

$$\begin{array}{ccccccc}
0 & \longrightarrow & P_1^{\oplus 3} & \xrightarrow{\psi_4} & P_2 \oplus P_3^{\oplus 2} & \xrightarrow{\phi_4} & P_4 \\
& & \Downarrow & & \Downarrow & & \Downarrow \\
& & (x, y, z) & \longmapsto & (-a_1y + a_2z, -ca_2x + by, ca_1x - bz) & \longmapsto & (du + g_1v + g_2w) \\
& & & & (u, v, w) & & \\
& & & & \longrightarrow & S_4 & \longrightarrow 0
\end{array}$$

to enhance the triangulated category  $D^b \text{ mod } \mathbb{C}\Gamma_4^{\rightarrow}$ . Here, the map  $\psi_4$  is chosen so that

$$\phi_4 \circ \psi_4(x, y, z) = \frac{\partial \Psi}{\partial f_1} x + \frac{\partial \Psi}{\partial f_2} y + \frac{\partial \Psi}{\partial f_3} z.$$

For example,  $\text{hom}_{\mathcal{A}}(S_2, S_3)$  is the total complex of the double complex

$$\begin{array}{ccc}
\text{Hom}(P_2, P_1 \oplus P_2) & \xrightarrow{\phi_3 \circ \bullet} & \text{Hom}(P_2, P_3) \\
\bullet \circ \phi_2 \downarrow & & \downarrow \bullet \circ \phi_2 \\
\text{Hom}(P_1^{\oplus 2}, P_1 \oplus P_2) & \xrightarrow{\phi_3 \circ \bullet} & \text{Hom}(P_1^{\oplus 2}, P_3).
\end{array}$$

The Ext-groups in  $D^b \text{ mod } \mathbb{C}\Gamma_4^{\rightarrow}$  are the cohomologies of the spaces of morphisms in  $\mathcal{A}$ ;

$$\text{Ext}^k(S_i, S_j) = H^k(\text{hom}_{\mathcal{A}}(S_i, S_j)).$$

From the above resolutions, one can easily see that

$$\dim \text{Ext}^k(S_i, S_j) = \begin{cases} 1 & k = 0 \text{ and } i = j, \\ \#\{\text{arrows of } \Gamma_4 \text{ from } v_j \text{ to } v_i\} & k = 1 \text{ and } i > j, \\ \#\{\text{arrows of } \Gamma_4 \text{ from } v_i \text{ to } v_j\} & k = 2 \text{ and } i > j, \\ 0 & \text{otherwise.} \end{cases}$$

The  $A_{\infty}$ -operations  $\mathbf{m}_k^{\mathcal{B}}$  of the minimal model  $\mathcal{B}$  can be computed by the homological perturbation theory [24, 19, 29, 28]. Let  $A = \bigoplus_{i,j=1}^4 \text{hom}_{\mathcal{A}}(S_i, S_j)$  be the total morphism differential graded algebra. Take a representative of  $B = \bigoplus_{i,j=1}^4 \text{Ext}^*(S_i, S_j) = H^*(A)$  and a direct sum decomposition  $A = B \oplus N_1 \oplus N_2$  so that  $\ker \mathbf{m}_1^A = B \oplus N_2$  and  $\mathbf{m}_1^A|_{N_1} : N_1 \xrightarrow{\sim} N_2$ . Let  $\pi : \ker d \rightarrow B$  be the projection and  $G : \ker d \rightarrow N_1$  be the projection to  $N_2$  composed with the inverse map of  $\mathbf{m}_1^A|_{N_1} : N_1 \xrightarrow{\sim} N_2$ . Then the  $A_{\infty}$ -operations  $\mathbf{m}_k^{\mathcal{B}}$  on  $B$  is defined by the sum over rooted trivalent trees;

$$\mathbf{m}_k^{\mathcal{B}} = \sum_T \mathbf{m}_{k,T}.$$

Here  $\mathbf{m}_{k,T}$  for a rooted tree  $T$  is defined as the composition of the product  $\mathbf{m}_2^A$  for each internal vertex, the map  $G$  for each internal edge and the projection  $\pi$  for the root edge. For example,

$$\begin{aligned} \mathbf{m}_1^B(x) &= 0, \\ \mathbf{m}_2^B(x, y) &= \pi \mathbf{m}_2^A(x, y), \\ \mathbf{m}_3^B(x, y, z) &= \pi \mathbf{m}_2^A(G\mathbf{m}_2^A(x, y), z) + \pi \mathbf{m}_2^A(x, G\mathbf{m}_2^A(y, z)), \\ \mathbf{m}_4(x, y, z, w) &= \pi \mathbf{m}_2^A(G\mathbf{m}_2^A(x, y), G\mathbf{m}_2^A(z, w)) + \pi(\mathbf{m}_2^A(G\mathbf{m}_2^A(G\mathbf{m}_2^A(x, y), z), w) \\ &\quad + \pi \mathbf{m}_2^A(G\mathbf{m}_2^A(x, G\mathbf{m}_2^A(y, z)), w) + \pi \mathbf{m}_2^A(x, G\mathbf{m}_2^A(G\mathbf{m}_2^A(y, z), w)) \\ &\quad + \pi \mathbf{m}_2^A(x, G\mathbf{m}_2^A(y, G\mathbf{m}_2^A(z, w))). \end{aligned}$$

Let us apply the above formula to compute  $\mathbf{m}_3^B(A_2, C, G_1)$ . Here,  $G_1 \in \text{hom}_{\mathcal{A}}^1(S_4, S_3)$  is defined by

$$\begin{array}{ccc} P_1^{\oplus 3} & \xrightarrow{\psi_4} & P_2 \oplus P_3^{\oplus 2} \xrightarrow{\phi_4} P_4 \\ \downarrow G_{1,1} & & \downarrow G_{1,2} \\ P_1 \oplus P_2 & \xrightarrow{\phi_3} & P_3, \end{array}$$

where

$$\begin{array}{ccc} G_{1,1} : & P_1^{\oplus 3} & \longrightarrow & P_1 \oplus P_2 \\ & \Downarrow & & \Downarrow \\ & (u, v, w) & \longmapsto & (v, -a_2u), \end{array}$$

and

$$\begin{array}{ccc} G_{1,2} : & P_2 \oplus P_3^{\oplus 2} & \longrightarrow & P_3 \\ & \Downarrow & & \Downarrow \\ & (x, y, z) & \longmapsto & y, \end{array}$$

$C \in \text{hom}_{\mathcal{A}}^1(S_3, S_2)$  is defined by

$$\begin{array}{ccc} P_1 \oplus P_2 & \xrightarrow{\phi_3} & P_3 \\ \downarrow C & & \\ P_1^{\oplus 2} & \xrightarrow{\phi_2} & P_2 \end{array}$$

where

$$\begin{array}{ccc} C : & P_1 \oplus P_2 & \longrightarrow & P_2 \\ & \Downarrow & & \Downarrow \\ & (x, y) & \longmapsto & y, \end{array}$$

$A_2 \in \text{hom}_{\mathcal{A}}^1(S_2, S_1)$  is defined by

$$\begin{array}{ccc} P_1^{\oplus 2} & \xrightarrow{\phi_3} & P_2 \\ \downarrow A_2 & & \\ P_1 & & \end{array}$$

where

$$\begin{array}{ccc} A_2 : & P_1^{\oplus 2} & \longrightarrow & P_1 \\ & \cup & & \cup \\ & (x, y) & \longmapsto & y. \end{array}$$

Then, the composition  $\mathbf{m}_2^A(C, G_1) = C \circ G_1 \in \text{hom}_{\mathcal{A}}^2(S_4, S_2)$  is given by

$$\begin{array}{ccccc} P_1^{\oplus 3} & \xrightarrow{\psi_4} & P_2 \oplus P_3^{\oplus 2} & \xrightarrow{\phi_4} & P_4 \\ \downarrow D & & & & \\ P_1^{\oplus 2} & \xrightarrow{\phi_2} & P_2 & & \end{array}$$

where

$$\begin{array}{ccc} D : & P_1^{\oplus 3} & \longrightarrow & P_2 \\ & \cup & & \cup \\ & (x, y, z) & \longmapsto & -a_2 y. \end{array}$$

If we define  $E \in \text{hom}_{\mathcal{A}}^1(S_4, S_2)$  by

$$\begin{array}{ccccc} P_1^{\oplus 3} & \xrightarrow{\psi_4} & P_2 \oplus P_3^{\oplus 2} & \xrightarrow{\phi_4} & P_4 \\ E_1 \downarrow & & \downarrow E_2=0 & & \\ P_1^{\oplus 2} & \xrightarrow{\phi_2} & P_2 & & \end{array}$$

where

$$\begin{array}{ccc} E_1 : & P_1^{\oplus 3} & \longrightarrow & P_1^{\oplus 2} \\ & \cup & & \cup \\ & (x, y, z) & \longmapsto & (0, -y), \end{array}$$

then we have

$$\mathbf{m}_1^A(E) = -dE = -E_2 \circ \psi_4 + \phi_2 \circ E_1 = D.$$

This shows that

$$\begin{aligned} \mathbf{m}_3^B(A_2, C, G_1) &= \pi \mathbf{m}_2^A(\text{Gm}_2^A(A_2, C), G_1) + \pi \mathbf{m}_2^A(A_2, \text{Gm}_2^A(C, G_1)), \\ &= \pi \mathbf{m}_2^A(0, G_1) + \pi \mathbf{m}_2^A(A_2, E) \in \text{hom}_B^2(S_4, S_1) \end{aligned}$$

is the map

$$\begin{array}{ccc} P_1^{\oplus 3} & \xrightarrow{\psi_4} & P_2 \oplus P_3^{\oplus 2} \xrightarrow{\phi_4} P_4. \\ \downarrow A_2 \circ E_1 & & \\ P_1 & & \end{array}$$

This  $A_\infty$ -operation corresponds to the term  $-g_1 c a_2 f_1$  in the potential  $\Phi$  in (6). In the same way, one can show that all the other  $A_\infty$ -operations of  $\mathcal{B}$  come from terms in the potential  $\Phi$ ; for a suitable choice of the basis

$$\begin{aligned} \mathrm{hom}_{\mathcal{B}}^1(S_4, S_3) &= \mathrm{span}\{G_1, G_2\}, \\ \mathrm{hom}_{\mathcal{B}}^1(S_4, S_2) &= \mathrm{span}\{D\}, \\ \mathrm{hom}_{\mathcal{B}}^2(S_4, S_1) &= \mathrm{span}\{F_1, F_2, F_3\}, \\ \mathrm{hom}_{\mathcal{B}}^1(S_3, S_2) &= \mathrm{span}\{C\}, \\ \mathrm{hom}_{\mathcal{B}}^1(S_3, S_1) &= \mathrm{span}\{B\}, \\ \mathrm{hom}_{\mathcal{B}}^1(S_2, S_1) &= \mathrm{span}\{A_1, A_2\}, \end{aligned}$$

the  $A_\infty$ -operations of the minimal model  $\mathcal{B}$  are given by

$$\begin{aligned} \mathfrak{m}_3(A_1, C, G_2) &= F_1, \\ \mathfrak{m}_3(A_2, C, G_1) &= -F_1, \\ \mathfrak{m}_2(B, G_1) &= F_2, \\ \mathfrak{m}_2(A_1, D) &= -F_2, \\ \mathfrak{m}_2(A_2, D) &= F_3, \\ \mathfrak{m}_2(B, G_2) &= -F_3, \end{aligned}$$

and zero otherwise.

## 7 The coamoeba and vanishing cycles for $\mathbb{P}^2$ blown-up at one point

Here we study the vanishing cycles of the mirror of  $X_4$  and their images by the argument map. Put

$$W_4(x, y) = x + y - \frac{1}{x} + \frac{1}{xy}.$$

The asymptotic boundary of the coamoeba of  $W_4^{-1}(0)$  coincides with the unique admissible configuration of lines in Figure 21. Unlike the cases of  $\mathbb{P}^2$

and  $\mathbb{P}^1 \times \mathbb{P}^1$  considered in [39, 40], the actual boundary of the coamoeba does not coincide with the asymptotic boundary. Figure 38 shows a schematic picture of the coamoeba.

The holomorphic map  $W_4$  has four critical points. Take the origin as the base point and let  $(c_i)_{i=1}^4$  be the distinguished set of vanishing paths, defined as the straight line segments from the origin to the critical values as in Figure 36. Consider the second projection

$$\begin{array}{ccc} \pi : W_4^{-1}(0) & \rightarrow & \mathbb{C}^\times \\ \cup & & \cup \\ (x, y) & \mapsto & y. \end{array}$$

The fiber  $\pi^{-1}(y)$  consists of two points for  $y \in \mathbb{C}^\times \setminus \{1\}$ , whereas  $\pi^{-1}(1)$  consists of only one point (the other point goes to  $x = 0$ ). Figure 37 shows the image by  $\pi$  of the distinguished basis  $(C_i)_{i=1}^4$  of vanishing cycles along the paths  $(c_i)_{i=1}^4$ . The black dots are the branch points, the white dots are  $y = 0$  and  $y = 1$ , the solid lines are the images of the vanishing cycles and the dotted lines are cuts introduced artificially to divide  $W_4^{-1}(0)$  into two sheets as shown in Figure 40 and Figure 41.

To study the image of the vanishing cycles by the argument map, we cut the coamoeba into pieces along the bold lines in Figure 39. These lines look as in Figure 40 and Figure 41 on the two sheets. They cut  $W_4^{-1}(0)$  into the union of two quadrilaterals and four triangles, glued along ten edges. By gluing these pieces, one obtains an elliptic curve minus four points in Figure 42. One can see that the vanishing cycles on  $W_4^{-1}(0)$  looks as in Figure 43 using Figures 37, 40, 41, and 42.

The dots on the vanishing cycles in Figure 43 show our choice of the branch points for the spin structures. One can also see that the images of the vanishing cycles by the argument map encircle the holes in the coamoeba as shown in Figure 44.

To show an equivalence between  $\mathfrak{Fuk}^\rightarrow W_4$  and the  $A_\infty$ -category  $\mathcal{B}$  introduced in section 6, identify the object  $C_i$  of  $\mathfrak{Fuk}^\rightarrow W_4$  with the object  $S_{5-i}$  of  $\mathcal{B}$  for  $i = 1, \dots, 4$ , and the morphisms  $A_1, A_2, B, \dots, F_3 \in \bigoplus_{i,j=1}^4 \text{hom}_{\mathcal{B}}(S_i, S_j)$  with the intersection points of vanishing cycles on the cuts  $a_1, a_2, b, \dots, f_3$  respectively. Note that the vertices of the brane tiling are in one-to-one correspondence with the holomorphic disks bounded by the vanishing cycles, which give  $A_\infty$ -operations in the directed Fukaya category. It is easy to see that these  $A_\infty$ -operations in  $\mathfrak{Fuk}^\rightarrow W$  are identical to those in  $\mathcal{B}$  appearing in section 6.

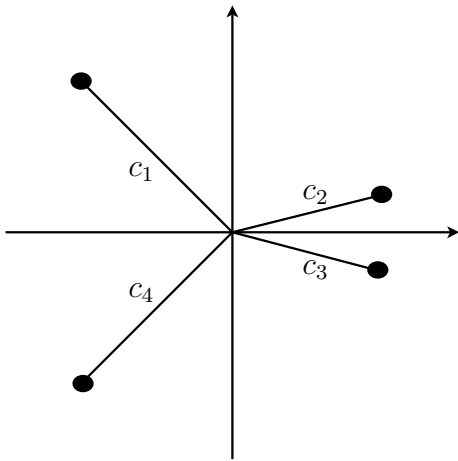


Figure 36: A distinguished basis of vanishing paths

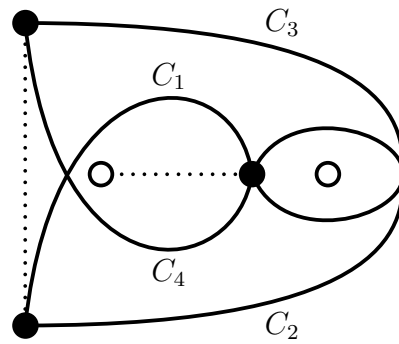


Figure 37: The images by  $\pi$  of the vanishing cycles

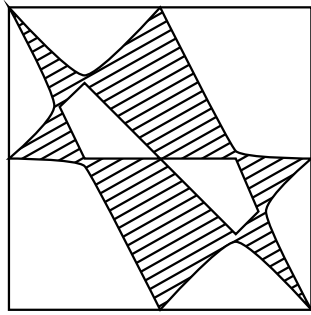


Figure 38: The coamoeba of  $W_4^{-1}(0)$

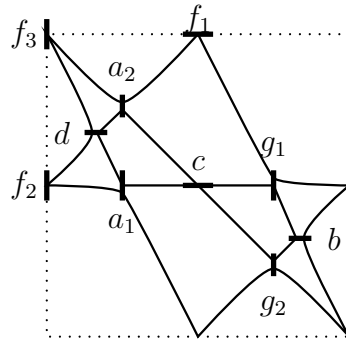


Figure 39: Cutting the coamoeba into pieces

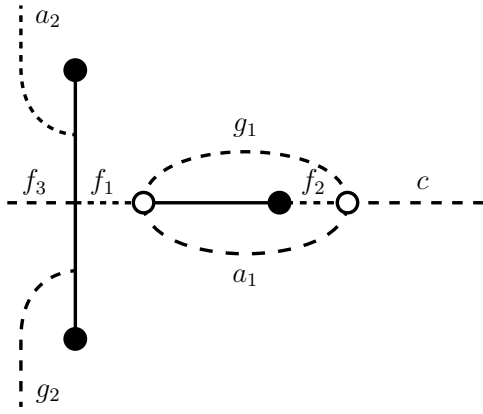


Figure 40: The first sheet of  $W_4^{-1}(0)$

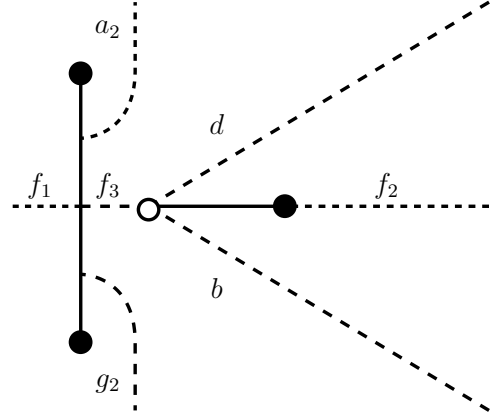


Figure 41: The second sheet of  $W_4^{-1}(0)$

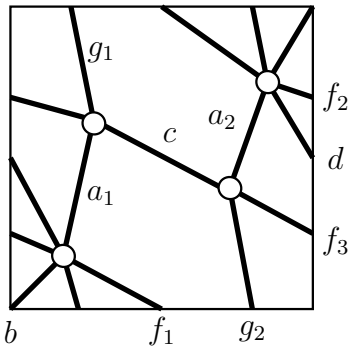


Figure 42: The glued surface

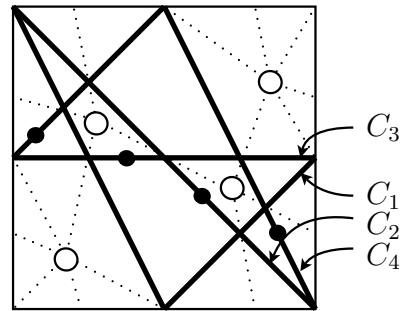


Figure 43: The vanishing cycles

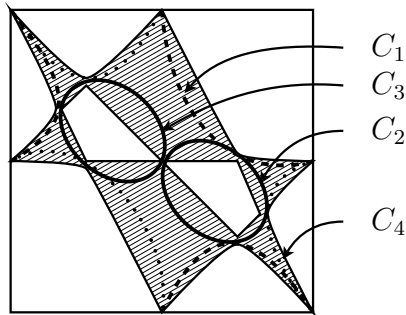


Figure 44: Vanishing cycles on the coamoeba

## 8 Toric orbifolds of $\mathbb{P}^2$ blown-up at one point

Here we discuss the quotient stack of  $X_4$  by the action of a finite subgroup of the torus. Let

$$P = \begin{pmatrix} p & q \\ r & s \end{pmatrix}$$

be an integer-valued matrix such that  $\det P \neq 0$ , and  $K \subset (\mathbb{C}^\times)^2$  be the kernel of the map

$$\begin{array}{ccc} P \otimes \mathbb{C}^\times : (\mathbb{C}^\times)^2 & \rightarrow & (\mathbb{C}^\times)^2 \\ \downarrow \Psi & & \downarrow \Psi \\ (x, y) & \mapsto & (x^p y^q, x^r y^s). \end{array}$$

Note that any finite subgroup of the torus  $(\mathbb{C}^\times)^2$  can be obtained in this way.

Now consider the quotient stack  $[X_4/K]$ . From the construction of toric stacks given in the introduction,  $[X_4/K]$  comes from the polygon  $P^T(\Delta_4)$ , i.e., the image of the polygon  $\Delta_4$  corresponding to  $X_4$  by the transpose of  $P$ . The brane tiling for the polygon  $P^T(\Delta_4)$  can be obtained from the brane tiling for  $\Delta_4$  by changing the periods; consider the universal cover of the brane tiling for  $\Delta_4$  in Figure 26, which is a periodic bipartite graph on  $\mathbb{R}^2$ , and take the quotient not by  $\mathbb{Z}^2$  but by  $P(\mathbb{Z}^2)$ . The configurations of lines corresponding to this brane tiling can be obtained as the asymptotic boundary of the coamoeba of the zero of the Laurent polynomial

$$(W_4 \circ (P \otimes \mathbb{C}^\times))(x, y) = x^p y^q + x^r y^s - \frac{1}{x^p y^q} + \frac{1}{x^{p+r} y^{q+s}}.$$

The critical points of  $W_4 \circ (P \otimes \mathbb{C}^\times)$  are the inverse images by  $P \otimes \mathbb{C}^\times$  of the critical points of  $W_4$ . Although some of the critical values of  $W_4 \circ (P \otimes \mathbb{C}^\times)$  coincide, it does not cause any problem in the definition of the directed Fukaya category since all the critical points are non-degenerate and the vanishing cycles corresponding to the same critical value do not intersect. The coamoeba of  $(W_4 \circ (P \otimes \mathbb{C}^\times))^{-1}(0)$  is obtained from the coamoeba of  $W_4^{-1}(0)$  by the same change-of-periods operation as the brane tiling, and it is clear that the relation between the directed Fukaya category and the brane tiling for  $W_4 \circ (P \otimes \mathbb{C}^\times)$  follows from that for  $W_4$ .

It follows from the definition that the category  $\text{coh}[X_4/K]$  of coherent sheaves on the quotient stack  $[X_4/K]$  is equivalent to the category  $\text{coh}^K X_4$  of  $K$ -equivariant coherent sheaves on  $X_4$ . It has a full strong exceptional

collection

$$\begin{aligned}
&(\mathcal{O} \otimes \rho_1, \mathcal{O} \otimes \rho_2, \dots, \mathcal{O} \otimes \rho_k, \\
&\quad \mathcal{O}(H - E) \otimes \rho_1, \dots, \mathcal{O}(H - E) \otimes \rho_k, \\
&\quad \mathcal{O}(H) \otimes \rho_1, \dots, \mathcal{O}(H) \otimes \rho_k, \\
&\quad \mathcal{O}(2H - E) \otimes \rho_0, \dots, \mathcal{O}(2H - E) \otimes \rho_k),
\end{aligned}$$

where  $(\mathcal{O}, \mathcal{O}(H - E), \mathcal{O}(H), \mathcal{O}(2H - E))$  is the full strong exceptional collection on  $X_4$  equipped with a suitable  $K$ -linearization and  $\{\rho_i\}_{i=1}^k$  is the set of irreducible representations of  $K$ . One can easily see that the total morphism algebra of the above full strong exceptional collection is isomorphic to the path algebra of the directed quiver with relations obtained from the one in Figure 32 by the change of periods. These facts suffice to prove homological mirror symmetry for the quotient stack  $[X_4/K]$ .

## 9 The case of $\mathbb{P}^2$ blown-up at two or three points

Here we discuss the case of  $\mathbb{P}^2$  blown-up at two or three points. Since most of the story is parallel to the case of  $\mathbb{P}^2$  blown-up at one point, we will be brief.

First we discuss the case of  $\mathbb{P}^2$  blown-up at two points. The corresponding lattice polygon  $\Delta_5$  together with the outward normal vectors is shown in Figure 45. In this case, there are 18 combinatorially distinct configurations of oriented lines, and only two of them shown in Figure 46 and Figure 47 are admissible. This non-uniqueness comes from the reflection symmetry of  $\Delta_5$  along the diagonal, and the resulting brane tilings are isomorphic. The configuration of lines in Figure 46 can be realized as the asymptotic boundary of the coamoeba of the zero of the Laurent polynomial

$$W_5(x, y) = \mathbf{e}(0.1)x + \mathbf{e}(-0.1)y + \frac{1}{x} + \frac{1}{xy} + \frac{1}{y}.$$

Figure 48 shows the corresponding brane tiling, and the resulting quiver is shown in Figure 50. Figure 49 shows the critical values of  $W_5$  and a distinguished basis of vanishing paths, which are just the straight line segments from the origin. The numbers on the vertices of the quiver in Figure 50 is chosen so that the vanishing cycle along the path  $c_i$  in Figure 49 corresponds to the  $i$ -th vertex for  $i = 1, \dots, 5$ . Since the rest of the story goes just the same way as in the case of  $\mathbb{P}^2$  blown-up at one point, we do not repeat it here.

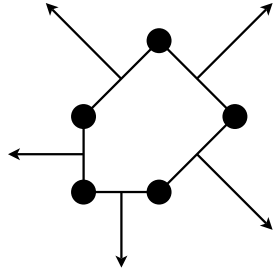


Figure 45: The lattice polygon  $\Delta_5$

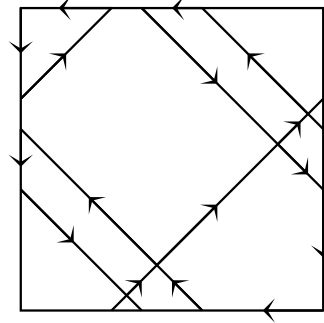


Figure 46: An admissible configuration of lines

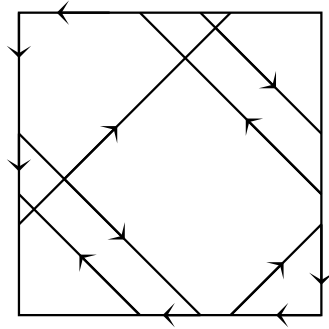


Figure 47: Another admissible configuration of lines

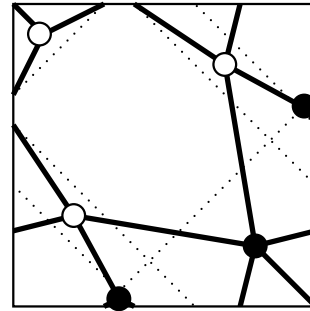


Figure 48: The brane tiling

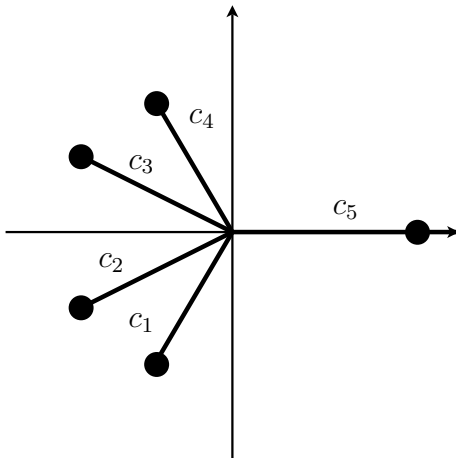


Figure 49: A distinguished set of vanishing paths

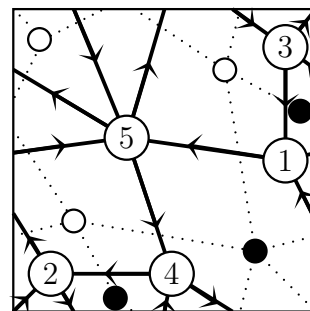


Figure 50: The quiver

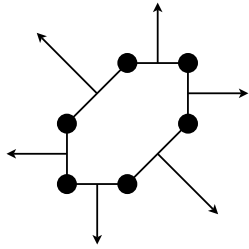


Figure 51: The lattice polygon  $\Delta_6$

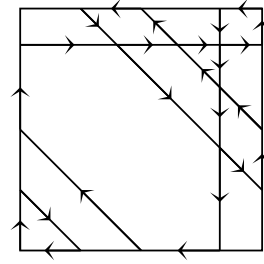


Figure 52: An admissible configuration of lines

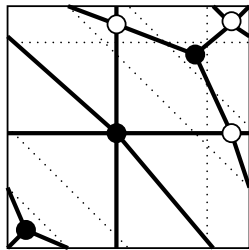


Figure 53: The brane tiling

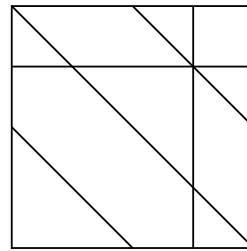


Figure 54: The asymptotic boundary

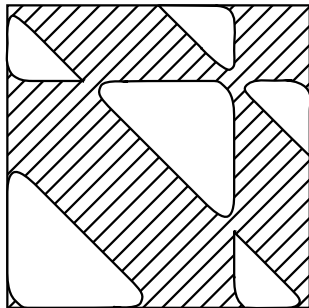


Figure 55: The coamoeba

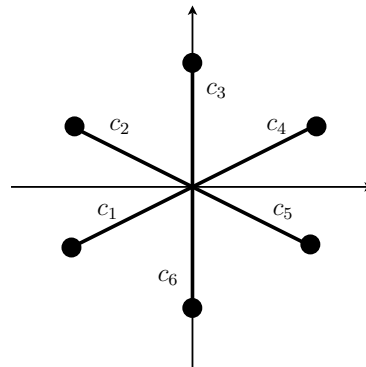


Figure 56: A distinguished set of vanishing paths

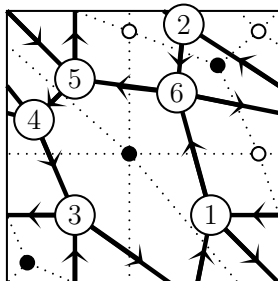


Figure 57: The quiver

Next we discuss the case of  $\mathbb{P}^2$  blown-up at three points. The corresponding lattice polygon  $\Delta_6$  together with the outward normal vectors is shown in Figure 51. Among 34 distinct configurations of oriented lines, we have two admissible ones, which lead to isomorphic brane tilings. In this case, it is impossible to realize an admissible configuration as the asymptotic boundary of a coamoeba. Nevertheless, the discussion in the previous sections goes through for the exact Lefschetz fibration defined by the Laurent polynomial

$$W_6(x, y) = -x - \sqrt{-1}xy - \sqrt{-1}y - \frac{\sqrt{-1}}{x} - \frac{\sqrt{-1}}{xy} + \frac{1}{y}.$$

The asymptotic boundary of the coamoeba of  $W_6^{-1}(0)$  is shown in Figure 54, and a schematic picture of the actual coamoeba is shown in Figure 55. Figure 56 shows the critical values of  $W_6$  and a distinguished set  $(c_i)_{i=1}^6$  of vanishing paths starting from the origin. Again we can cut the coamoeba into pieces and use the second projection  $W_6^{-1}(0) \ni (x, y) \mapsto y \in \mathbb{C}^\times$  as in section 7 to show that the image of the vanishing cycle along the path  $c_i$  encircles the hole in the coamoeba corresponding to the  $i$ -th vertex of the quiver in Figure 57. The rest of the story goes just the same way.

## References

- [1] Mohammed Abouzaid. Homogeneous coordinate rings and mirror symmetry for toric varieties. [math.SG/0511644](#), 2005.
- [2] Mohammed Abouzaid. Morse homology, tropical geometry, and homological mirror symmetry for toric varieties. [math.SG/0610004](#), 2006.
- [3] Denis Auroux, Ludmil Katzarkov, and Dmitri Orlov. Mirror symmetry for weighted projective planes and their noncommutative deformations. [math.AG/0404281](#), 2004.
- [4] Denis Auroux, Ludmil Katzarkov, and Dmitri Orlov. Mirror symmetry for Del Pezzo surfaces: Vanishing cycles and coherent sheaves. [math.AG/0506166](#), 2005.
- [5] A. A. Beilinson. Coherent sheaves on  $\mathbf{P}^n$  and problems in linear algebra. *Funktsional. Anal. i Prilozhen.*, 12(3):68–69, 1978.
- [6] A. I. Bondal. Representations of associative algebras and coherent sheaves. *Izv. Akad. Nauk SSSR Ser. Mat.*, 53(1):25–44, 1989.

- [7] A. I. Bondal and M. M. Kapranov. Enhanced triangulated categories. *Mat. Sb.*, 181(5):669–683, 1990.
- [8] Tom Bridgeland.  $t$ -structures on some local Calabi-Yau varieties. *J. Algebra*, 289(2):453–483, 2005.
- [9] Manfred Einsiedler, Mikhail Kapranov, and Douglas Lind. Non-archimedean amoebas and tropical varieties. *math.AG/0408311*, 2004.
- [10] Bo Feng, Yang-Hui He, Kristian D. Kennaway, and Cumrun Vafa. Dimer models from mirror symmetry and quivering amoebae. *hep-th/0511287*, 2005.
- [11] Andreas Floer. Morse theory for Lagrangian intersections. *J. Differential Geom.*, 28(3):513–547, 1988.
- [12] Andreas Floer. A relative Morse index for the symplectic action. *Comm. Pure Appl. Math.*, 41(4):393–407, 1988.
- [13] Sebastián Franco, Amihay Hanany, Dario Martelli, James Sparks, David Vegh, and Brian Wecht. Gauge theories from toric geometry and brane tilings. *J. High Energy Phys.*, (1):128, 40 pp. (electronic), 2006.
- [14] Sebastián Franco, Amihay Hanany, David Vegh, Brian Wecht, and Kristian D. Kennaway. Brane dimers and quiver gauge theories. *J. High Energy Phys.*, (1):096, 48 pp. (electronic), 2006.
- [15] Kenji Fukaya. Morse homotopy,  $A^\infty$ -category, and Floer homologies. In *Proceedings of GARC Workshop on Geometry and Topology '93 (Seoul, 1993)*, volume 18 of *Lecture Notes Ser.*, pages 1–102, Seoul, 1993. Seoul Nat. Univ.
- [16] Kenji Fukaya. Floer homology and mirror symmetry. II. In *Minimal surfaces, geometric analysis and symplectic geometry (Baltimore, MD, 1999)*, volume 34 of *Adv. Stud. Pure Math.*, pages 31–127. Math. Soc. Japan, Tokyo, 2002.
- [17] Kenji Fukaya, Yong-Geun Oh, Hiroshi Ohta, and Kaoru Ono. Lagrangian intersection Floer theory. preprint available at <http://www.math.kyoto-u.ac.jp/~fukaya/>.
- [18] Victor Ginzburg. Calabi-Yau algebras. *math.AG/0612139*, 2006.

- [19] V. K. A. M. Gugenheim, L. A. Lambe, and J. D. Stasheff. Perturbation theory in differential homological algebra. II. *Illinois J. Math.*, 35(3):357–373, 1991.
- [20] Amihay Hanany, Christopher P. Herzog, and David Vegh. Brane tilings and exceptional collections. hep-th/0602041, 2006.
- [21] Amihay Hanany and Kristian D. Kennaway. Dimer models and toric diagrams. hep-th/0503149, 2005.
- [22] Amihay Hanany and David Vegh. Quivers, tilings, branes and rhombi. hep-th/0511063, 2005.
- [23] K. Jung and D. van Straten. Arctic computation of monodromy. to appear in *Oberwolfach Reports*.
- [24] T. V. Kadeishvili. The algebraic structure in the homology of an  $A(\infty)$ -algebra. *Soobshch. Akad. Nauk Gruzin. SSR*, 108(2):249–252 (1983), 1982.
- [25] Gabriel D. Kerr. Weighted blowups and mirror symmetry for toric surfaces. math.AG/0609162, 2006.
- [26] Maxim Kontsevich. Homological algebra of mirror symmetry. In *Proceedings of the International Congress of Mathematicians, Vol. 1, 2 (Zürich, 1994)*, pages 120–139, Basel, 1995. Birkhäuser.
- [27] Maxim Kontsevich. Lectures at ENS Paris, spring 1998. set of notes taken by J. Bellaïche, J.-F. Dat, I. Martin, G. Rachinet and H. Randriambololona, 1998.
- [28] Maxim Kontsevich and Yan Soibelman. Homological mirror symmetry and torus fibrations. In *Symplectic geometry and mirror symmetry (Seoul, 2000)*, pages 203–263. World Sci. Publishing, River Edge, NJ, 2001.
- [29] S. A. Merkulov. Strong homotopy algebras of a Kähler manifold. *Internat. Math. Res. Notices*, (3):153–164, 1999.
- [30] Grigory Mikhalkin. Decomposition into pairs-of-pants for complex algebraic hypersurfaces. *Topology*, 43(5):1035–1065, 2004.
- [31] Mikael Passare and Hans Rullgård. Amoebas, Monge-Ampère measures, and triangulations of the Newton polytope. *Duke Math. J.*, 121(3):481–507, 2004.

- [32] A. N. Rudakov. Exceptional collections, mutations and helices. In *Helices and vector bundles*, volume 148 of *London Math. Soc. Lecture Note Ser.*, pages 1–6. Cambridge Univ. Press, Cambridge, 1990.
- [33] Kyoji Saito. Around the theory of the generalized weight system: relations with singularity theory, the generalized Weyl group and its invariant theory, etc. [ MR0855023 (88c:32015a); MR0876442 (88c:32015b)]. In *Selected papers on harmonic analysis, groups, and invariants*, volume 183 of *Amer. Math. Soc. Transl. Ser. 2*, pages 101–143. Amer. Math. Soc., Providence, RI, 1998.
- [34] Paul Seidel. Graded Lagrangian submanifolds. *Bull. Soc. Math. France*, 128(1):103–149, 2000.
- [35] Paul Seidel. Vanishing cycles and mutation. In *European Congress of Mathematics, Vol. II (Barcelona, 2000)*, volume 202 of *Progr. Math.*, pages 65–85. Birkhäuser, Basel, 2001.
- [36] Paul Seidel. More about vanishing cycles and mutation. In *Symplectic geometry and mirror symmetry (Seoul, 2000)*, pages 429–465. World Sci. Publishing, River Edge, NJ, 2001.
- [37] Paul Seidel. Homological mirror symmetry for the quartic surface. math.AG/0310414, 2003.
- [38] Kazushi Ueda. Homological mirror symmetry for toric del Pezzo surfaces. *Comm. Math. Phys.*, 264(1):71–85, 2006.
- [39] Kazushi Ueda and Masahito Yamazaki. A note on brane tilings and McKay quivers. math.AG/0605780, 2006.
- [40] Kazushi Ueda and Masahito Yamazaki. Brane tilings for parallelograms with application to homological mirror symmetry. math.AG/0606548, 2006.

Kazushi Ueda

Department of Mathematics, Graduate School of Science, Osaka University, Machikaneyama 1-1, Toyonaka, Osaka, 560-0043, Japan.

*e-mail address* : kazushi@cr.math.sci.osaka-u.ac.jp

Masahito Yamazaki

Department of Physics, School of Science, The University of Tokyo, Hongo 7-3-1, Bunkyo-ku, Tokyo, 113-0033, Japan

*e-mail address* : yamazaki@hep-th.phys.s.u-tokyo.ac.jp